AMERICAN SOCIETY FOR MICROBIOLOGY | Journal of Bacteriology®

RESEARCH ARTICLE

The $TonB_m$-PocAB System Is Required for Maintenance of Membrane Integrity and Polar Position of Flagella in *Pseudomonas putida*

Kadi Ainsaar,[a] Hedvig Tamman,[a] Sergo Kasvandik,[b] Tanel Tenson,[b] Rita Hõrak[a]

[a]Institute of Molecular and Cell Biology, University of Tartu, Tartu, Estonia
[b]Institute of Technology, University of Tartu, Tartu, Estonia

ABSTRACT TonB-ExbB-ExbD-like energy transduction systems are widespread among Gram-negative bacteria. While most species have only one copy of *tonB-exbBD* genes, the *Pseudomonas* species possess more TonB-ExbBD homologues. One of them, the TonB3-PocA-PocB complex, was recently shown to be required for polar localization of FlhF and, thus, the flagella in *Pseudomonas aeruginosa*. Here, we show that the orthologous $TonB_m$-PocA-PocB complex is important for polar localization of FlhF and flagella in *Pseudomonas putida* as well. Additionally, the system is necessary for maintaining membrane integrity, as the inactivation of the $TonB_m$-PocAB complex results in increased membrane permeability, lowered stress tolerance, and conditional cell lysis. Interestingly, the functionality of $TonB_m$-PocAB complex is more important for stationary than for exponentially growing bacteria. The whole-cell proteome analysis provided a likely explanation for this growth phase dependence, as extensive reprogramming was disclosed in an exponentially growing $tonB_m$ deletion strain, while only a few proteomic changes, mostly downregulation of outer membrane proteins, were determined in the stationary-phase $\Delta tonB_m$ strain. We propose that this response in exponential phase, involving, *inter alia*, activation of AlgU and ColR regulons, can compensate for $TonB_m$-PocAB's deficiency, while stationary-phase cells are unable to alleviate the lack of $TonB_m$-PocAB. Our results suggest that mislocalization of flagella does not cause the membrane integrity problems; rather, the impaired membrane intactness of the $TonB_m$-PocAB-deficient strain could be the reason for the random placement of flagella.

IMPORTANCE The ubiquitous *Pseudomonas* species are well adapted to survive in a wide variety of environments. Their success relies on their versatile metabolic, signaling, and transport ability but also on their high intrinsic tolerance to various stress factors. This is why the study of the stress-surviving mechanisms of *Pseudomonas* species is of utmost importance. The stress tolerance of *Pseudomonads* is mainly achieved through the high barrier property of their membranes. Here, we present evidence that the TonB-ExbBD-like $TonB_m$-PocAB system is involved in maintaining the membrane homeostasis of *Pseudomonas putida*, and its deficiency leads to lowered stress tolerance and conditional cell lysis.

KEYWORDS flagellum localization, growth phase dependence, membrane homeostasis, stress tolerance, swimming motility, whole-cell proteome

The cell envelope of Gram-negative bacteria contains two membranes separated by a periplasmic space (1). Due to cell envelope architecture, no energy is produced in the outer membrane, which means that transport proteins that require energy need to import it from the cytoplasmic membrane. The energy transfer is carried out by the TonB-ExbB-ExbD complex in the inner membrane that harnesses the proton motive

Citation Ainsaar K, Tamman H, Kasvandik S, Tenson T, Hõrak R. 2019. The $TonB_m$-PocAB system is required for maintenance of membrane integrity and polar position of flagella in *Pseudomonas putida*. J Bacteriol 201:e00303-19. https://doi.org/10.1128/JB.00303-19.

Editor Victor J. DiRita, Michigan State University

Address correspondence to Rita Hõrak, rita.horak@ut.ee.

Received 27 April 2019
Accepted 7 June 2019
Accepted manuscript posted online 10 June 2019
Published 8 August 2019

force and directly interacts with the TonB-dependent transporters in the outer membrane (2, 3). Once thought to be restricted only to iron and vitamin B_{12} transport, the TonB-ExbBD complex promotes the transport of a wide range of substrates that are too large or scarce to enter the cell by diffusion (4).

The TonB-ExbBD system is intensively studied in *Escherichia coli*, but the exact mechanism of its functioning in energy transduction has remained unclear. TonB and ExbD each have a transmembrane N terminus and are predominantly located in the periplasm, whereas ExbB has three transmembrane domains and a large cytoplasmic domain. ExbB forms a proton channel (5) and provides the structure for the complex (6). Depending on the membrane condition, ExbB proteins form either a pentameric or a hexameric channel with different conductance for protons (7). ExbD is predicted to be the carrier of protons during their translocation from periplasm to cytoplasm (8), but ExbD also interacts with TonB and appears to determine the right conformation of TonB during energy transmission (9, 10). TonB expands across the periplasm and transduces the harvested energy to the outer membrane transporters (11, 12) that have a TonB box domain. This domain is proposed to extend into the periplasm and become available for interaction with TonB after the binding of substrate to the transporter (13).

The TonB-ExbBD complexes are widespread among Gram-negative bacteria. Most species, including *E. coli*, have one copy of *tonB-exbBD* genes, but the number of *tonB* homologues can vary by up to nine per genome (14). The ubiquitous soil and rhizosphere bacterium *Pseudomonas putida* possesses two TonB homologues encoded by PP_4994 and PP_5308. PP_5308 (*tonB*) is in an operon with *exbB* and *exbD*, and their corresponding proteins appear to have a function similar to that of their *E. coli* homologs, as the *P. putida* strains defective in *tonB-exbBD* genes are impaired in siderophore transport and deficient in iron acquisition (15, 16). Moreover, the *exbB* of *P. putida* can complement the lack of *exbB* in *E. coli* (15). Besides its importance in iron transport, the TonB-ExbBD complex is required for *P. putida* for the tolerance of several antibiotics, *p*-hydroxybenzoate, and toluene (16, 17) and affects its fitness in colonizing corn seeds and roots (18).

PP_4994 has not been studied in *P. putida*, but its conserved homologues can be found in most *Pseudomonas* species (19). The orthologue of PP_4994 in *P. aeruginosa*, TonB3, likely forms an inner membrane-associated complex with homologues of ExbB and ExbD, named PocA and PocB, respectively (20). Interestingly, *P. aeruginosa*'s TonB3-PocAB complex does not appear to have a role in promoting iron transport (21). Instead, it is involved in swimming and twitching ability (20, 22). The TonB3-PocAB complex, although not polarly localized itself, is needed for the polar localization of flagella and type IV pili (20). Deleting any one of the *tonB3-pocAB* genes in *P. aeruginosa* reduces swimming due to the random localization of flagella, which is caused by the random localization of otherwise polarly localized FlhF protein.

In this study, we investigate the role of PP_4994-encoded TonB and PP_1898-1899-encoded PocAB in *P. putida*. We show that like its orthologue in *P. aeruginosa*, the TonB-PocAB complex of *P. putida* is needed for correct placement of flagella and FlhF. For this shared role in motility, we name the PP_4994-encoded protein $TonB_m$. Interestingly, our results also indicate that the $TonB_m$-PocAB complex has a separate task in maintaining membrane integrity. The $TonB_m$-PocAB-deficient strains have permeable membranes and are sensitive to several chemicals. Curiously, the effects of $TonB_m$-PocAB's deficiency depend on the physiological state of the inoculum as bacteria originating from stationary phase are significantly more compromised than the exponentially growing $TonB_m$-PocAB knockout mutants. The comparison of whole-cell proteomes of the Δ*tonB*$_m$ strain and wild-type *P. putida* revealed extensive proteomic changes occurring in the exponentially growing but not in the stationary-phase Δ*tonB*$_m$ strain. We hypothesize that the observed changes compensate for the lack of *tonB*$_m$ in exponentially growing cells.

RESULTS

Inactivation of the $TonB_m$-PocAB complex decreases swimming and results in membrane defects. The ability of bacteria to bind Congo red (CR) dye has been used

as a marker of membrane defects and cell lysis (23). Thus, we screened a transposon mutant library of the *P. putida* wild-type strain for CR binding mutants to find genes that could be important in membrane homeostasis. In accordance with previous studies (23, 24), the current screen repeatedly detected the CR binding mutants with transposon insertion into the *colRS* operon. ColR is the response regulator of the ColRS two-component regulatory system that responds to the excess of metals, such as zinc, iron, manganese, and cadmium (25). In the absence of this system, *P. putida* has problems with maintaining cell membrane integrity not only in the presence of excess metals (25, 26) but also on glucose minimal medium (23, 24). The second most common cause of pink colonies was disruption of PP_4994, which codes for an orthologue of *P. aeruginosa*'s TonB3. For one pink colony, the transposon had disrupted PP_1898, a probable orthologue of *P. aeruginosa*'s *pocA* gene (19). Identifying orthologues of genes that regulate flagellum localization in *P. aeruginosa* (20) in our membrane stress screen was intriguing, because assuming that PP_4994 and PocA of *P. putida* have functions similar to those of their orthologues, it is unclear why wrong localization of flagella and decreased motility result in membrane stress (23, 24).

To get further insight into the role(s) of PP_4994 and PocAB in *P. putida*, the PP_4994 (*tonB$_m$*), PP_1898 (*pocA*), and PP_1899 (*pocB*) single deletion strains as well as the whole TonB$_m$-PocAB complex deletion strain (Δ*tonB$_m$* Δ*pocAB*) were constructed. As the decreased swimming ability of *P. aeruginosa* in the absence of the TonB3-PocAB system is caused by the nonpolar localization of FlhF (20), a protein that determines the place of flagellum formation (27), the *flhF* (PP_4343) deletion strain was constructed as well.

To test if *tonB$_m$*, *pocA*, and *pocB* are required for motility in *P. putida*, the swimming ability of all the deletion strains was analyzed. Compared to the Δ*flhF* strain, which had a severe motility defect, the swimming ability of Δ*tonB$_m$*, Δ*pocA*, Δ*pocB*, and Δ*tonB$_m$* Δ*pocAB* strains was less affected but nevertheless clearly inhibited (Fig. 1A). The Δ*tonB$_m$* Δ*flhF* double deletion strain displayed swimming defects similar to that of the Δ*flhF* strain, which is in good correlation with FlhF lying downstream of the TonB3-PocAB system in regulation of flagellum localization in *P. aeruginosa* (20). Complementation of the Δ*tonB$_m$* strain with ectopically expressed *tonB$_m$* restored normal motility (Fig. 1A).

To determine if the swimming defect of TonB$_m$-PocAB- and FlhF-deficient strains is caused by incorrect localization of flagella, the position of flagella was ascertained by microscopy. More than 90% of exponentially growing wild-type *P. putida* cells had all of their flagella (1 to 5 flagella) located at the center of the cell pole (Fig. 1B and C). However, in the TonB$_m$-PocAB single and triple deletion strains, the uniform polar placement of flagella was lost and approximately 80% to 90% of cells had at least one incorrectly placed flagellum (Fig. 1B and C). The Δ*flhF* and Δ*tonB$_m$* Δ*flhF* mutants had a random distribution of flagella similar to that of TonB$_m$-PocAB-deficient strains (Fig. 1C), and their number of flagella per cell was decreased. Already without isopropyl-β-D-thiogalactopyranoside (IPTG) induction, the *tonB$_m$* complementation strain showed more cells with only polar flagella (35%), which indicates that the *tac* promoter in the *lacI*^{q}-P$_{tac}$-*tonB$_m$* cassette was leaky. When the expression of TonB$_m$ was induced with 0.5 mM IPTG, about 80% of the cells of the *tonB$_m$* complementation strain had polar flagella (Fig. 1C). To analyze the localization of FlhF, the *flhF-gfp* translational fusion was constructed and introduced into the chromosome of *P. putida* wild-type, Δ*tonB$_m$*, Δ*flhF*, and Δ*tonB$_m$* Δ*flhF* strains. Fluorescence microscopy showed that FlhF-green fluorescent protein (FlhF-GFP) is polar in wild-type and Δ*flhF* strains but locates randomly in Δ*tonB$_m$* and Δ*tonB$_m$* Δ*flhF* strains (Fig. 1D). We also observed that the FlhF-GFP foci were brighter in wild-type and Δ*flhF* bacteria than in the *tonB$_m$*-deficient bacteria, where more FlhF-GFP seemed to localize in the cytoplasm. Thus, our data indicate that the *P. putida* TonB$_m$-PocAB system has a role similar to that of TonB3-PocAB in *P. aeruginosa*.

To investigate whether the motility defect and random localization of flagella correlate with the CR-binding phenotype, the motility-deficient strains were tested on glucose medium supplemented with CR. Interestingly, while strains with the TonB$_m$-PocAB-deficient system stained pink, the Δ*flhF* strain resembled wild-type *P. putida*

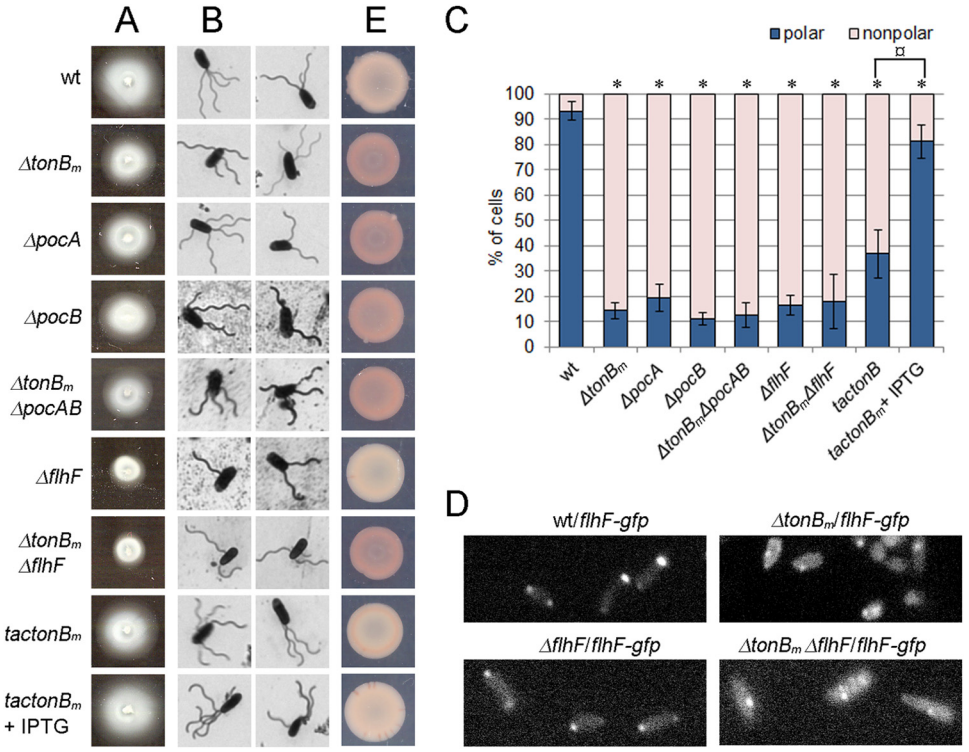

FIG 1 Effect of $TonB_m$-PocAB system's deficiency in swimming ability (A), flagellum localization (B and C), FlhF positioning (D), and Congo red binding (E). The cells of *P. putida* wild type (wt), *tonB*$_m$, *pocA*, *pocB*, and *flhF* single deletion strains, *tonB*$_m$ *pocAB* triple deletion strain, *tonB*$_m$ *flhF* double deletion strain, and *tonB*$_m$ deletion strain complemented with the *tonB*$_m$ gene (*tac tonB*$_m$) and wild-type, Δ*tonB*$_m$, Δ*flhF*, and Δ*tonB*$_m$ Δ*pocAB* strains carrying the *flhF-gfp* fusion under the control of the inducible P_{tac} promoter were grown at 30°C. The expression of $TonB_m$ and FlhF-GFP was induced with 0.5 mM IPTG. (A) Swimming ability. The cells were grown on LB medium containing 0.3% agarose for 18 h. (B) Localization of flagella. Exponentially growing cells (OD_{580} of ~0.5) were stained with silver and examined using oil immersion light microscopy. (C) Quantification of flagellum localization. Flagellum localization was considered random (nonpolar) if at least one flagellum deviated from polar positioning. Relative proportions of cells with polar and nonpolar flagella (means with 95% confidence intervals from at least four independent experiments) are presented. Two hundred to 800 cells were examined for each strain. Statistically significant differences from the wild type (*, $P < 0.001$) and difference from the uninduced *tac tonB*$_m$ strain (¤, $P = 0.000003$) are indicated. (D) Localization of FlhF-GFP. The cells were grown overnight in LB medium supplemented with IPTG and examined using oil immersion light microscopy. (E) Congo red (CR) binding. The cells were grown on glucose minimal medium supplemented with 0.0005% CR for 72 h.

(Fig. 1E). The control experiment with the *tonB*$_m$ complementation strain revealed that the CR binding phenotype of the Δ*tonB*$_m$ strain is suppressed by the overexpression of $TonB_m$. These data show that the motility defect and wrong localization of flagella do not account for the CR binding of the Δ*tonB*$_m$, Δ*pocA*, and Δ*pocB* strains and that in the absence of $TonB_m$-PocAB system, cells must have additional problems not related to the misplacement of flagella.

The absence of $TonB_m$-PocAB complex results in glucose-specific cell lysis. Given that the Congo red binding indicates a severe membrane defect (23, 24), we next tested the motility mutants for membrane leakage. We introduced the β-galactosidase expression plasmid into the wild-type and mutant strains and measured the β-galactosidase activity from the supernatant of glucose-grown bacteria. High extracellular β-galactosidase activity was detected in the case of Δ*tonB*$_m$, Δ*pocA*, Δ*pocB*, Δ*tonB*$_m$ Δ*pocAB*, and Δ*tonB*$_m$ Δ*flhF* strains, indicating cell lysis (Fig. 2A). Contrary to this finding, the Δ*flhF* mutant displayed no β-galactosidase leakage.

In order to test whether the lysis of the Δ*tonB*$_m$, Δ*pocA*, and Δ*pocB* strains is dependent on the growth medium, the β-galactosidase leakage assay was performed with lysogeny broth (LB)-grown bacteria as well. However, as neither of the LB-grown strains differed from the wild type (Fig. 2A), the cell lysis of Δ*tonB*$_m$, Δ*pocA*, and Δ*pocB* strains seems to be specific to growth on glucose.

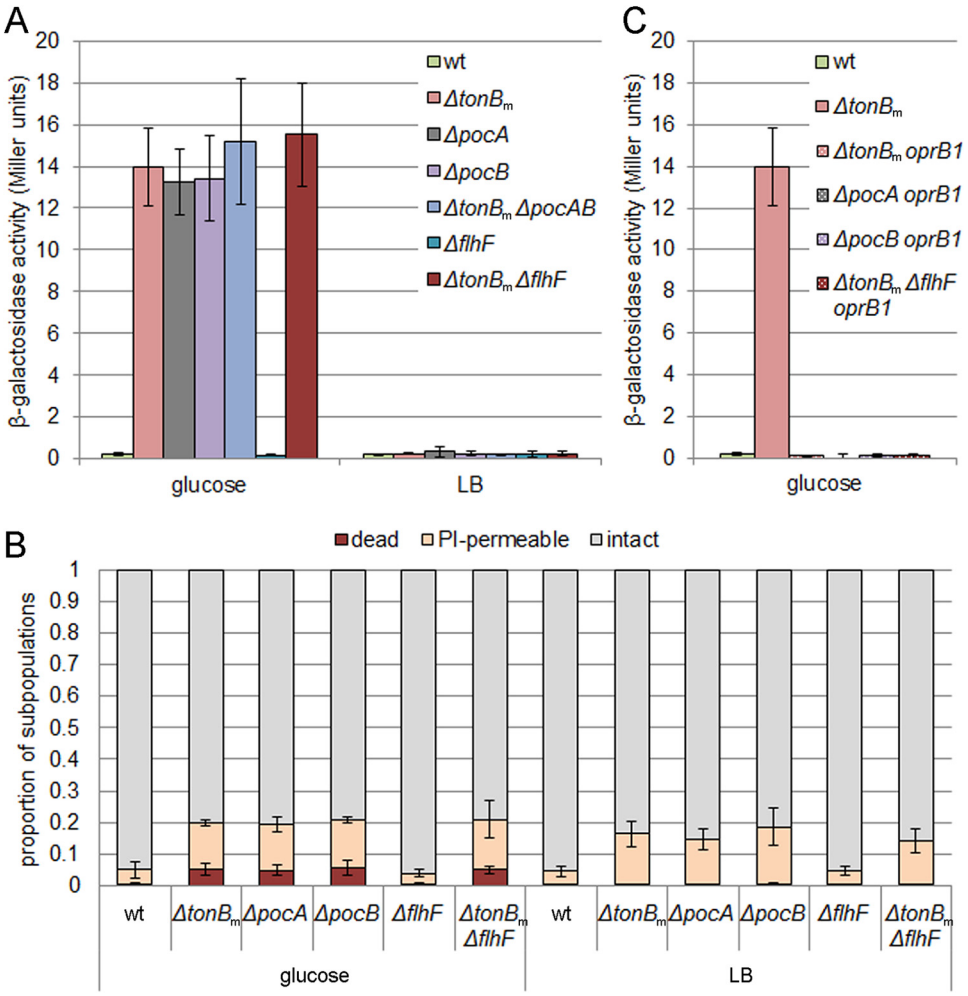

FIG 2 TonB$_m$-PocAB-deficient strains have increased membrane permeability. (A) β-Galactosidase activities measured from the supernatant of glucose- and LB-grown *P. putida* wt, *tonB$_m$*, *pocA*, *pocB*, and *flhF* single deletion, *tonB$_m$ pocAB* triple deletion, and *tonB$_m$ flhF* double deletion strains. All strains carry pKTlacZS/C plasmid. Data (means with 95% confidence intervals) from at least three independent experiments are presented. (B) Flow cytometry analysis of glucose- and LB-grown bacteria stained with SYTO9 and propidium iodide (PI). Relative proportions of the subpopulations of intact, PI-permeable, and dead cells (means with 95% confidence intervals) from at least four independent determinations are presented. (C) β-Galactosidase activities measured from the supernatant of glucose-grown *P. putida* wt, *tonB$_m$* deletion, *oprB1*-deficient *tonB$_m$*, and *pocA*, *pocB*, *flhF*, and *tonB$_m$ flhF* deletion strains. All strains carry pKTlacZS/C plasmid. Data (means with 95% confidence intervals) from at least three independent experiments are presented.

Previous results with *colR*-deficient *P. putida* have shown that glucose-specific cell lysis is a subpopulation phenotype (24, 28). Therefore, to get insight into the population structure of TonB$_m$-PocAB-deficient strains, flow cytometry analysis of bacteria stained with SYTO9 and propidium iodide (PI) was performed. Three populations could be detected: (i) undamaged cells that stained with SYTO9 only; (ii) cells that stained with both SYTO9 and PI (indicated as PI-permeable); and (iii) cells that stained with PI and SYTO9 but had lower side scatter. The latter subpopulation has been shown to correlate with cell lysis and therefore has been defined as dead cells (28). The single-cell analysis of the glucose solid medium-growing bacteria revealed that colonies of the Δ*tonB$_m$*, Δ*pocA*, Δ*pocB*, and Δ*tonB$_m$* Δ*flhF* strains contained more PI-permeable and dead cells than the wild type, whereas the deletion of *flhF* did not influence either the membrane permeability or death of bacteria (Fig. 2B). Interestingly, analysis of the mutants grown on LB solid medium also showed that the Δ*tonB$_m$*, Δ*pocA*, Δ*pocB*, and Δ*tonB$_m$* Δ*flhF* colonies contain more PI-permeable cells, but the amount of dead cells was similar to that of the wild type (Fig. 2B). The LB-grown Δ*flhF* strain had no difference from the wild

type. These results show that while the deficiency in the $TonB_m$-PocAB system increases membrane permeability regardless of the growth medium, the membrane damage is more pronounced on the glucose minimal medium. The unaffected membrane permeability of the Δ*flhF* strain indicates that wrong placement of flagella does not affect membrane permeability or cause cell lysis.

The inability to tolerate the increased expression of the sugar channel protein OprB1 in the outer membrane has been described as the reason for glucose-specific cell lysis in the *colR*-deficient mutant (23). To test if the glucose-induced OprB1 could be the reason for cell lysis of glucose-grown Δ*tonB*$_m$, Δ*pocA*, Δ*pocB*, and Δ*tonB*$_m$ Δ*flhF* cells as well, *oprB1*-deficient derivatives were constructed from the deletion strains and β-galactosidase leakage was analyzed. Data shown in Fig. 2C indicated that disruption of *oprB1* eliminated the glucose-dependent cell lysis of $TonB_m$-PocAB-deficient strains. This indicated that, similar to the *colR*-deficient mutant, glucose-induced expression of OprB1 was involved in the glucose-specific cell lysis of $TonB_m$-PocAB mutants.

$TonB_m$-PocAB system affects stress tolerance and generation time in a growth phase-dependent manner. Since the flow cytometry analysis revealed that the $TonB_m$-PocAB system contributes to membrane integrity, we hypothesized that the stress tolerance of these strains is affected. To test this, the growth of the Δ*tonB*$_m$, Δ*pocA*, and Δ*pocB* strains and wild-type *P. putida* was compared on LB medium supplemented with different chemicals: metal salts (LiCl, NaCl, $MnSO_4$, $FeSO_4$, $CoCl_2$, $NiSO_4$, $CuSO_4$, $ZnSO_4$, RbCl, $CdSO_4$, and $K_2Cr_2O_2$), antibiotics (colistin, polymyxin B, benzylpenicillin, tetracycline, and rifampin), DNA-damaging chemicals (mitomycin C and 4-nitroquinoline 1-oxide), compounds producing reactive oxygen species (paraquat and H_2O_2), and EDTA. The Δ*flhF* strain was used as a control to rule out the effect of mislocalization of flagella on stress tolerance. During the experiments we observed that the results were dependent on the age of the inoculum; thus, the stress tolerance of cells from both stationary and exponential growth phases was analyzed. When the exponential-phase cells were tested, difference in growth could be observed only on media containing $MnSO_4$ or 4-nitroquinoline 1-oxide (nitroquinoline) (Fig. 3A). However, when inoculated cells originated from the stationary growth phase, the $TonB_m$-PocAB deletion strains revealed increased sensitivity to $CuSO_4$, $MnSO_4$, colistin, benzylpenicillin, nitroquinoline, and mitomycin C (Fig. 3B), and their growth was slightly decreased by $ZnSO_4$, NaCl, and EDTA (data not shown). These results indicated that the $TonB_m$-PocAB complex affected *P. putida*'s stress tolerance, but the magnitude of the effect depended extensively on the growth phase. Given that the Δ*flhF* strain resembled that of the wild type under all conditions, the increased stress sensitivity could not be caused by mislocalization of flagella. Although the $TonB_m$-PocAB system was not involved in iron tolerance, we also investigated the growth of mutants under iron-limited conditions, but as no differences from the wild-type were detected (data not shown), the $TonB_m$-PocAB complex is likely not involved in iron acquisition.

To further analyze the growth phase effects of $TonB_m$-PocAB-deficient *P. putida*, the LB medium was inoculated with bacteria of different ages and growth curves were recorded. While the maximum growth rate of the wild type remained the same independent of the inoculum used, the growth rates of $TonB_m$-PocAB-deficient strains were clearly affected by the growth stage of the inoculum. When exponential-phase cells were used for inoculation, the growth curves and minimal generation times of Δ*tonB*$_m$, Δ*pocA*, and Δ*pocB* strains resembled those of the wild type (Fig. 3C). However, when the culture was started with stationary-phase cells, the minimal generation time for the Δ*tonB*$_m$ and Δ*pocAB* strains was, on average, about 10 min longer (Fig. 3D) and had a statistically significant difference from the wild type. This furthermore demonstrates that the effect of $TonB_m$-PocAB deficiency depends on the age of the *P. putida* cells.

MexCD-OprJ efflux system is downregulated in Δ*tonB*$_m$ strain in stationary phase. Considering that the $TonB_m$-PocAB system's homologue in *E. coli*, the TonB-ExbBD complex, connects the two membranes by mediating the energy of cytoplasmic membrane to outer membrane transporters (2), we next analyzed different membrane

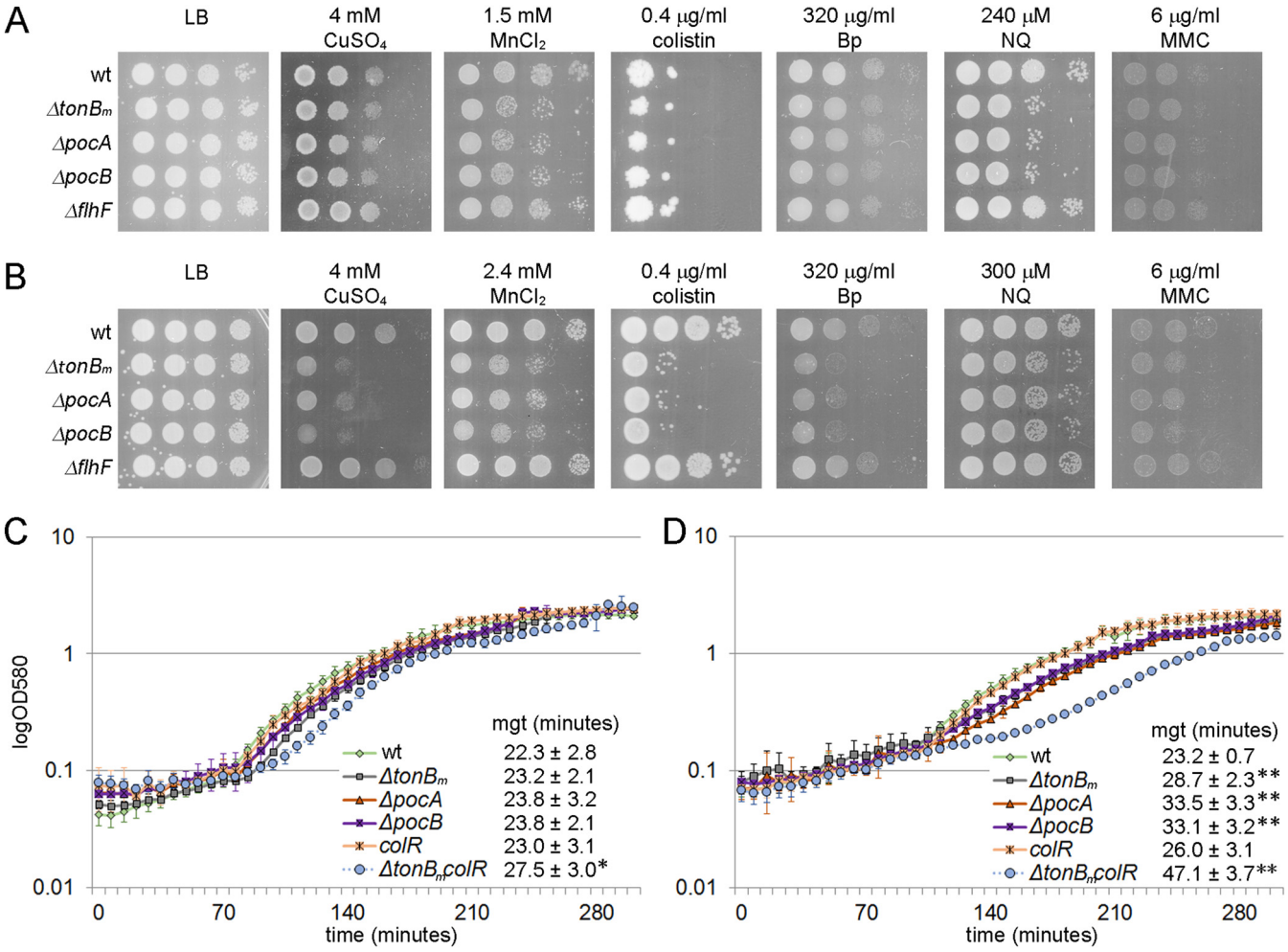

FIG 3 TonB$_m$-PocAB system affects stress tolerance and generation time in a growth phase-dependent manner. (A and B) Stress tolerance of exponential-phase (A) and stationary-phase (B) *P. putida* wt and *tonB$_m$*, *pocA*, *pocB*, and *flhF* deletion strains. Exponential-phase cells were grown for 3 h (OD_{580} of ~1) and stationary-phase cells overnight before inoculating the strains onto LB medium supplemented with different chemicals. The cells were then grown for 20 h at 30°C. Approximately 50,000, 5,000, 500, and 50 cells were inoculated per spot. Bp, benzylpenicillin; NQ, nitroquinoline; MMC, mitomycin C. (C and D) Growth curves and minimal generation times of bacterial cultures inoculated either with exponential-phase (C) or stationary-phase (D) cells. *P. putida* wt, *tonB$_m$*, *pocA*, and *pocB* deletion strains and *colR*-deficient and *tonB$_m$ colR* double deficient strains were grown for 3 h (exponential phase) or overnight (stationary phase) before inoculating the cells into LB medium. The strains were grown at 30°C on a microtiter plate. Means from eight parallels of one measurement with 95% confidence intervals are presented. Average minimal generation times (mgt) from three independent measurements for each strain also are shown. Statistically significant differences from the wild type are indicated (*, $P = 0.012$; **, $P < 0.0001$).

fractions of the TonB$_m$-PocAB-deficient strains from both exponential and stationary growth phases. While the patterns of lipopolysaccharides and periplasmic and cytoplasmic membrane proteins of wild-type and TonB$_m$-PocAB deletion strains were similar (data not shown), the outer membrane protein (OMP) pattern of mutants revealed noticeable differences from the wild type (Fig. 4).

To get more detailed insight into the protein profile of the TonB$_m$-deficient strain, a whole-cell proteome analysis of exponential- and stationary-phase Δ*tonB$_m$* and wild-type *P. putida* cells was performed. Extensive growth phase-dependent proteome rearrangements were detected in both strains: 1,426 proteins out of 2,652 in the wild-type strain (see Table S1 in the supplemental material) and 1,326 proteins out of 2,673 in the Δ*tonB$_m$* strain (Table S2) had a statistically significant and at least 2-fold difference between the growth phases. Interestingly, when the stationary-phase data of the wild type was compared to the corresponding Δ*tonB$_m$* data, only six proteins were found to be significantly differentially expressed (Fig. 5 and Table S3). Besides these six proteins, we also considered nine differentially expressed proteins that were present in

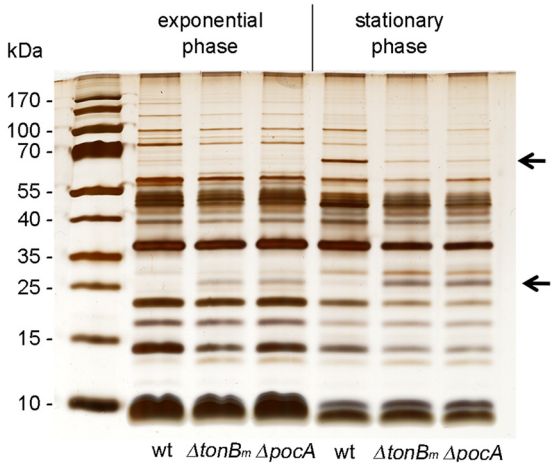

FIG 4 The absence of intact $TonB_m$-PocAB complex causes changes in the outer membrane protein pattern. Outer membrane proteins were prepared from *P. putida* wt and $tonB_m$ and *pocA* deletion strains, separated by SDS-PAGE, and visualized by silver staining. Cells were grown in LB medium for 3 h (OD_{580} of ~1; exponential phase) or 17 h (stationary phase). All lanes contain 1 μg of protein. Major differences between wild-type and $tonB_m$-*pocAB*-deficient strains are indicated by arrows.

all the samples of one strain but were not detectable in any of the parallels of the other (so-called on-off-regulated proteins) and had at least a 2-fold difference in their expression level when imputed values were used. Notably, 11 of these 15 were membrane proteins, most of them being downregulated in the Δ$tonB_m$ strain (Fig. 5 and Table S3). The greatest differences were the 20-, 82-, and 65-fold decreases in the

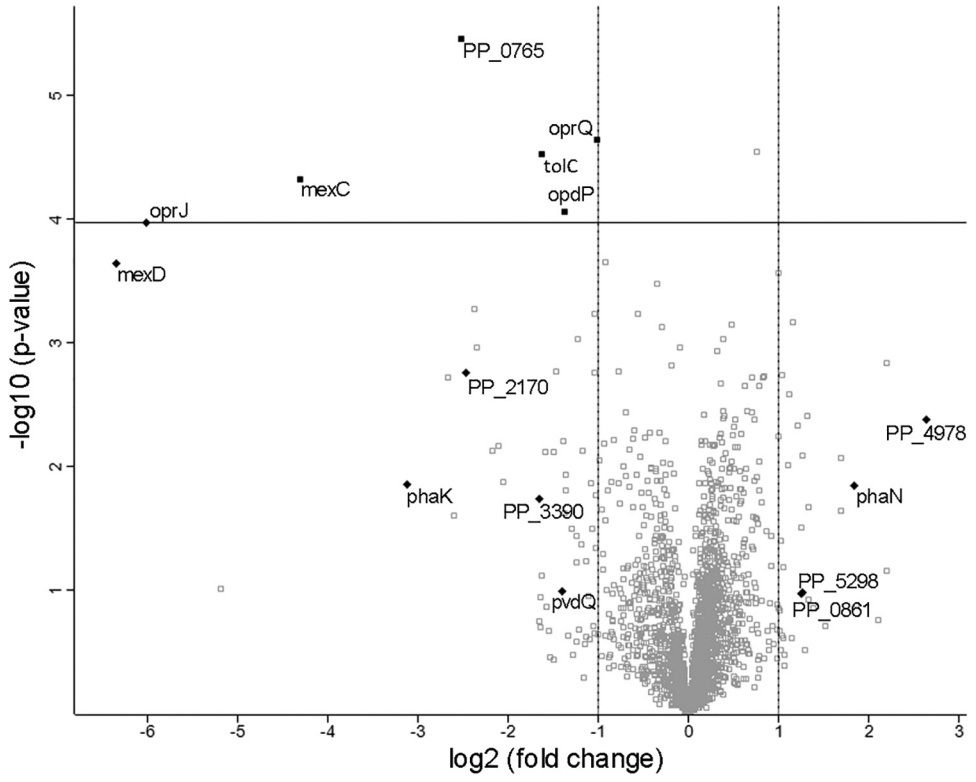

FIG 5 Volcano plot showing differences in protein expression between stationary-phase $tonB_m$-deficient *P. putida* and the wild type. Filled symbols represent 15 proteins considered differently expressed in the Δ$tonB_m$ strain. Diamonds indicate on-off-regulated proteins. Proteins located above the horizontal line have statistically significant changes in their expression values.

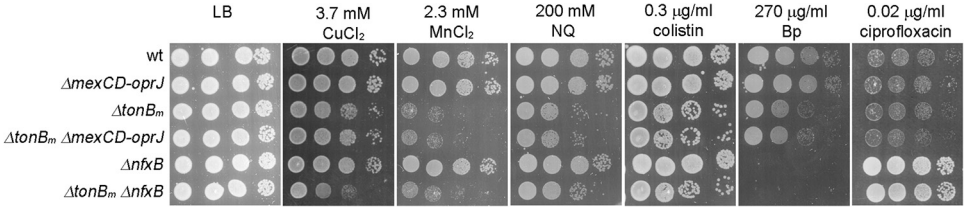

FIG 6 MexCD-OprJ effux pump is not related to the stress susceptibility of *tonB$_m$* deletion strain. Overnight-grown *P. putida* wt, *mexCD-oprJ*, *tonB$_m$*, and *nfxB* deletion strains and *tonB$_m$ mexCD-oprJ* and *tonB$_m$ nfxB* double deletion strains were grown on LB medium supplemented with different chemicals for 20 h at 30°C. Approximately 50,000, 5,000, 500, and 50 cells were inoculated per spot.

amount of MexC, MexD, and OprJ, respectively, which together form a multidrug efflux system that exports several antimicrobial agents in *P. aeruginosa* (29). The level of PhaK, an outer membrane channel protein that facilitates the uptake of phenylacetic acid (30), had dropped about 9-fold. This is probably caused by the 4-fold increased level of PhaN, a transcriptional repressor of the phenylacetic acid pathway (30).

In wild-type cells, MexCD-OprJ efflux pump components are upregulated in stationary phase (Table S1), whereas in the Δ*tonB$_m$* strain, MexC is clearly downregulated and MexD and OprJ are not even detectable in stationary phase (Tables S2 and S3). This remarkable downregulation of MexCD-OprJ efflux pump proteins in the Δ*tonB$_m$* strain led us to hypothesize that it was the reason for the decreased stress tolerance of the Δ*tonB$_m$* strain. To test this possibility, we deleted the whole *mexCD-oprJ* operon from both wild-type and Δ*tonB$_m$* strains and tested stress tolerance. The deletion of *mexCD-oprJ* had no effect on the tolerance of $CuSO_4$, $MnSO_4$, nitroquinoline, colistin, benzylpenicillin (Fig. 6), polymyxin B, and mitomycin C (data not shown) in either of the strains, suggesting that MexCD-OprJ did not contribute to the efflux of these compounds and that the downregulation of MexCD-OprJ complex was not the cause of elevated stress sensitivity of the Δ*tonB$_m$* strain. On the other hand, if the MexCD-OprJ complex was related to the stress tolerance of the Δ*tonB$_m$* strain, then its overexpression should have alleviated the increased sensitivity.

In *P. aeruginosa*, the expression of the *mexCD-oprJ* operon is controlled by two repressors, NfxB (31) and EsrC (32). The loss of NfxB leads to overexpression of *mexCD-oprJ* genes (33), whereas EsrC is active as a repressor only in the presence of NfxB and its effect on *mexCD-oprJ* is modest compared to that of NfxB (32). The homologue of NfxB in *P. putida* is PP_2820, and, expecting its absence to raise the expression of *mexCD-oprJ*, we constructed Δ*nfxB* (PP_2820) deletion strains of wild-type and Δ*tonB$_m$* strains. In *P. aeruginosa*, the upregulation of MexCD-OprJ due to the loss of NfxB results in increased ciprofloxacin resistance (34). In accordance with that, the ciprofloxacin resistance of the Δ*nfxB* and Δ*tonB$_m$* Δ*nfxB* strains was considerably higher than that of their parent strains (Fig. 6), suggesting that MexCD-OprJ was upregulated in the *P. putida* Δ*nfxB* strain. To assess if increased expression of MexCD-OprJ would relieve the reduced stress tolerance of the Δ*tonB$_m$* strain, we next tested the Δ*nfxB* strain tolerance to several compounds. The results revealed that while the lack of *nfxB* decreased the benzylpenicillin tolerance of both wild-type and Δ*tonB$_m$* strains (Fig. 6), it did not influence the tolerance to other chemicals. These results support the contention that low levels of MexCD-OprJ are not sufficient to explain the decreased stress tolerance of the TonB$_m$-PocAB-deficient strain.

Proteome analysis revealed extensive changes in exponentially growing Δ*tonB$_m$* cells. Contrary to the few differences in stationary phase, the proteome analysis of exponential-phase cells showed at least a 2-fold change of 126 proteins in the Δ*tonB$_m$* strain compared to level for the wild type (Fig. 7 and Table S4). One hundred eight of these changes were statistically significant, but we also included 18 on-off proteins (Table S4). It is remarkable that most of the proteins, 102 out of 126, were upregulated in the Δ*tonB$_m$* strain (Fig. 7 and Table S4). Only the outer membrane proteins that predominantly belonged to the transport and secretion category were mainly down-

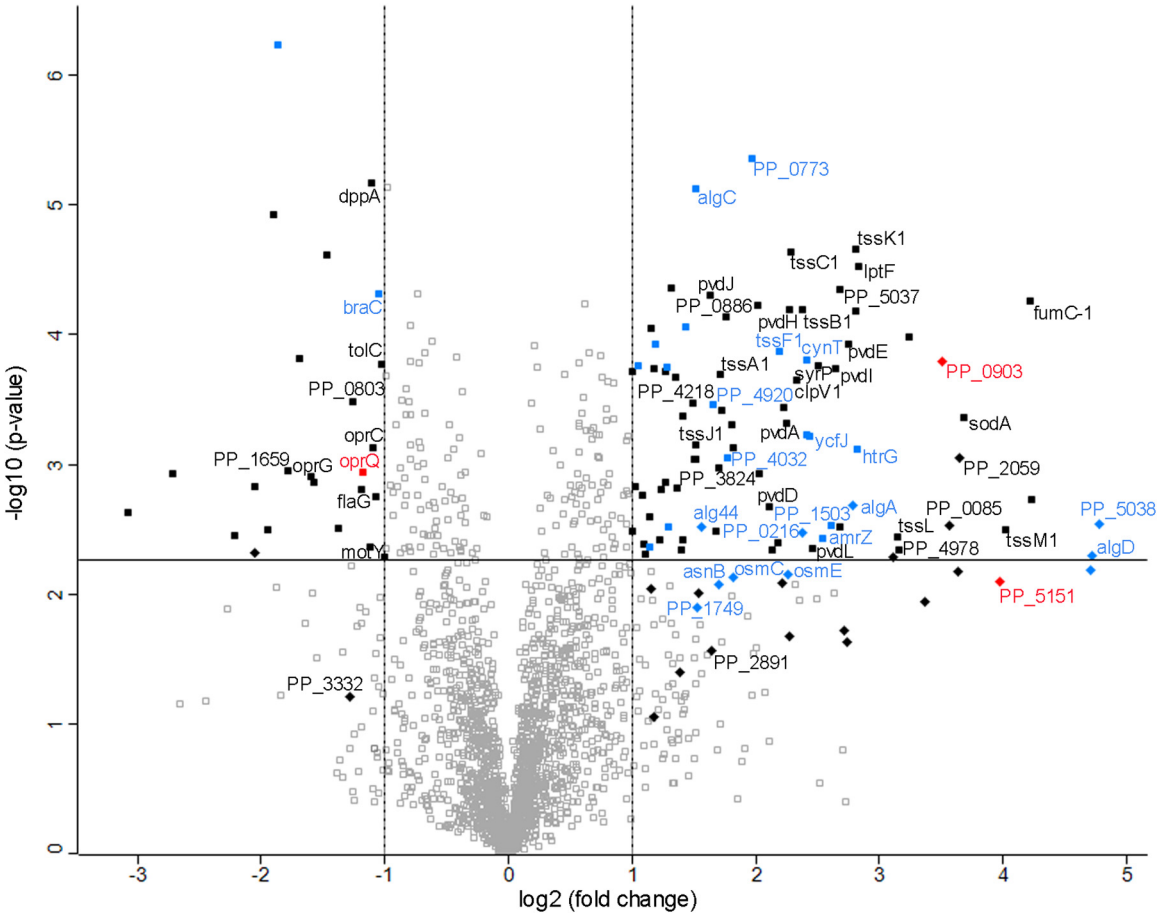

FIG 7 Volcano plot showing differences in protein expression between exponentially growing $tonB_m$-deficient *P. putida* and the wild type. Filled symbols represent 126 proteins considered differently expressed in the Δ$tonB_m$ strain. Diamonds indicate on-off proteins. Proteins belonging to the AlgU regulon are shown in blue, and proteins regulated by ColR are in red. A name tag indicates that the protein was also differently expressed in the zinc-exposed *colR*-deficient strain or is ColR regulated (also in red). Proteins located above the horizontal line have statistically significant changes in their expression values.

regulated. About a third of all the changed proteins were associated with either amino acid and protein metabolism (17 proteins) or with general metabolism (22 proteins), suggesting that a considerable metabolic reprogramming was induced in the exponentially growing Δ$tonB_m$ strain. Another large group comprised 29 proteins related to transport and secretion. Half of these proteins were downregulated in the Δ$tonB_m$ strain and half, including 10 proteins of the type VI secretion system K1 (35), were upregulated (Table S4). It is also noteworthy that 13 proteins associated with stress and defense responses and 10 transcriptional regulators or histidine kinases were responding to $TonB_m$ deficiency, and again, most of them were upregulated. Surprisingly, only five proteins (OprQ, OpdP, TolC, PP_0765, and PP_4978) overlapped the differentially expressed proteins of stationary phase.

AlgU and ColR regulons are activated in Δ$tonB_m$ strain. The proteome data of exponential-phase bacteria revealed that several alginate biosynthesis proteins as well as the alginate regulator AmrZ were upregulated in the Δ$tonB_m$ strain (Fig. 7 and Table S4). These results were verified by analysis of *amrZ-lacZ* and *algD-lacZ* transcriptional fusions in the Δ$tonB_m$ strain, showing an increased promoter activity (Fig. 8A and B). Alginate is an exopolysaccharide that contributes to biofilm formation and stress tolerance under water-limiting conditions in *P. putida* (36). In *P. aeruginosa*, alginate is produced in response to cell wall stress due to the activation of sigma factor AlgU (37). Analysis of the proteome response of the Δ$tonB_m$ strain revealed that 31 out of 126 differentially expressed proteins were orthologues of the *P. aeruginosa* AlgU regulon

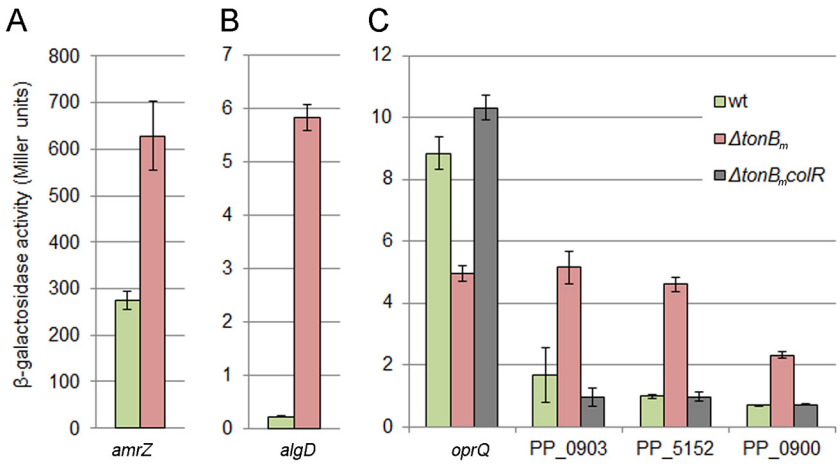

FIG 8 AlgU and ColR regulon genes respond to *tonB$_m$* deficiency. (A and B) β-Galactosidase activities measured in *P. putida* wt and *tonB$_m$* deletion strains carrying the *amrZ* or *algD* transcriptional fusion with *lacZ* in the plasmid p9TT$_B$lacZ. (C) β-Galactosidase activities measured in *P. putida* wt, *tonB$_m$* deletion, and *colR*-deficient *tonB$_m$* deletion strains carrying the *oprQ*, *PP_0903*, *PP_5152*, or *PP_0900* transcriptional fusion with *lacZ*. Bacteria were grown in LB medium for 3 h (OD$_{580}$ of ~1) at 30°C. Data (means with 95% confidence intervals) from at least four independent experiments are presented.

(Fig. 7, marked with blue) (37). This suggests that the AlgU regulon is activated in the exponentially growing Δ*tonB$_m$* strain.

Besides activation of the AlgU regulon, three proteins of the ColR regulon, OprQ, PP_0903, and PP_5151 (25), responded to TonB$_m$ deficiency (Fig. 7, indicated in red) in a direction indicating that the ColRS signaling is active in the Δ*tonB$_m$* strain. To test this possibility, the ColR-responsive *oprQ-lacZ*, *PP_0903-lacZ*, and *PP_5152-lacZ* transcriptional fusions (PP_5152 is the first gene in the two-gene PP_5152-PP_5151 operon) were analyzed in exponentially grown wild-type, Δ*tonB$_m$*, and Δ*tonB$_m$ colR* double mutant strains (Fig. 8C). The expression of *oprQ* is known to be repressed, and the expression of PP_0903 and PP_5152 activated by ColR (25, 38). In accordance with that and verifying the changes seen in the proteome data (Fig. 7), the promoter activity of *oprQ* was lower and the activities of PP_0903 and PP_5152 were higher in the Δ*tonB$_m$* than the wild-type strain (Fig. 8C). Given that none of the three promoters responded to the lack of *tonB$_m$* in the Δ*tonB$_m$ colR* strain (Fig. 8C), ColR is clearly responsible for the altered expression of those genes in the Δ*tonB$_m$* strain. To further confirm if ColRS signaling is active in TonB$_m$-PocAB-deficient cells, the expression of the ColR-responsive PP_0900, which was not detectable in the proteome, was also analyzed. Corroborating the prior results, the *PP_0900-lacZ* fusion was induced in TonB$_m$-deficient cells in a ColR-dependent manner (Fig. 8C), confirming the activation of the ColRS system in response to TonB$_m$-PocAB deficiency.

Activation of the ColR regulon is beneficial for the Δ*tonB$_m$* strain. The proteome of *colR*-deficient *P. putida* recently has been analyzed (26), and the comparison of these previous data to the current data revealed a remarkable overlap between the proteome responses of exponentially grown Δ*tonB$_m$* and zinc-stressed *colR* mutant strains (26). The same 61 proteins, including, for example, several transport and stress response proteins, were differentially expressed in both mutant strains, and all in the same manner (Fig. 7 [the overlapping 61 proteins are indicated with name tags] and Table S4). Considering this partial overlap of the proteome responses and several shared membrane stress-indicating phenotypes (glucose-induced Congo red binding and cell lysis) of Δ*tonB$_m$* and *colR* mutant cells (Fig. 1 and 2) (23), it was hypothesized that the activation of ColRS signaling could alleviate the membrane damage of the Δ*tonB$_m$* mutant. To test this, the growth parameters and stress tolerance of the Δ*tonB$_m$ colR* double mutant was analyzed. The growth curve of the combined mutant in LB medium displayed a prolonged lag phase that was particularly apparent when stationary-phase

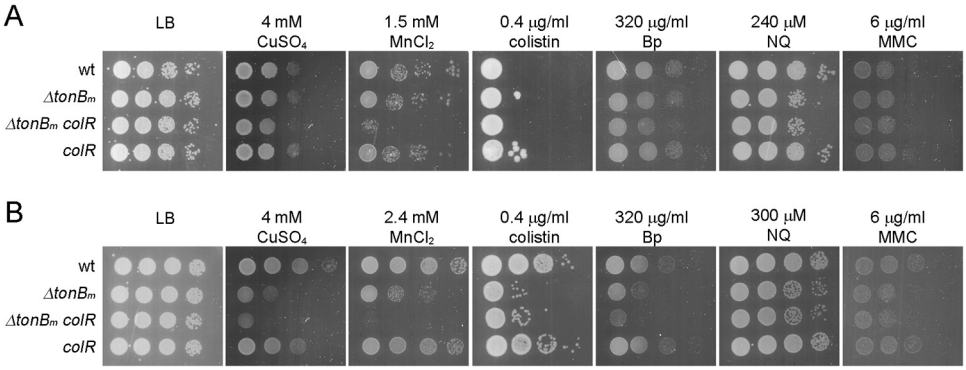

FIG 9 Stress tolerance of exponential-phase (A) and stationary-phase (B) *P. putida* wt, $tonB_m$ deletion, *colR*-deficient $tonB_m$ deletion, and *colR*-deficient strains. Exponential-phase cells were grown for 3 h (OD_{580} of ~1) and stationary-phase cells overnight before inoculating the strains onto LB medium supplemented with different chemicals. The cells were then grown for 20 h at 30°C. Approximately 50,000, 5,000, 500, and 50 stationary-phase cells were inoculated per spot.

cells were used as an inoculum (Fig. 3C and D). The minimal generation time of the Δ$tonB_m$ *colR* strain was, on average, about 5 min longer than that of other strains when exponential-phase cells were analyzed (Fig. 3C). The growth rate reduction of the double mutant was even more pronounced when stationary-phase inocula were tested (Fig. 3D). The Δ$tonB_m$ *colR* double mutant was also more compromised in some stress tolerance tests. Exponential-phase Δ$tonB_m$ *colR* cells were less tolerant to $MnCl_2$ than the $tonB_m$ single mutant (Fig. 9A), and the stationary-phase Δ$tonB_m$ *colR* double mutant tolerated less $CuSO_4$, $MnCl_2$, and benzylpenicillin than the Δ$tonB_m$ strain (Fig. 9B). Given that *colR* deficiency clearly intensifies the phenotypes of the Δ$tonB_m$ strain, the activation of the ColR regulon seems to be beneficial to *P. putida* lacking $TonB_m$. The accumulation of the effects of $tonB_m$ and *colR* deficiency suggests that the origin of the problems in these strains is different, which implies that although the lack of $TonB_m$-PocAB and ColRS produces similar responses, the two systems operate in separate regulatory pathways.

DISCUSSION

Prior to the current work, the homologue of the $TonB_m$-PocAB complex, TonB3-PocAB, was shown to be required for swimming and twitching in *P. aeruginosa* (20, 22). In the absence of *tonB3*, *pocA*, or *pocB*, the swimming ability of *P. aeruginosa* is impaired because the polar localization of flagella is lost due to the random positioning of FlhF (20), which marks the assembly point of new flagella (27). The present study suggests that the TonB-PocAB complex has the same function in other *Pseudomonas* species, as *P. putida* $tonB_m$, *pocA*, and *pocB* deletion strains have randomly distributed flagella and decreased swimming ability as well. However, our results indicate that besides the role in motility, the $TonB_m$-PocAB complex is needed for the maintenance of membrane integrity. We show that the misplacement of flagella is not responsible for the membrane defects of $TonB_m$-PocAB mutants and rather suggests that the impaired membrane homeostasis is the main cause for the random localization of flagella as well as for other deficiencies.

The subpopulation lysis of $TonB_m$-PocAB mutants on glucose medium, evidenced by the leakage of cytoplasmic β-galactosidase (Fig. 2A), clearly shows that these mutants have a fragile membrane. The finding that glucose-specific cell lysis was abolished by the deletion of *oprB1* indicates that $TonB_m$-PocAB-deficient strains cannot tolerate OprB1 porin. OprB1 is a carbohydrate-selective porin that has a relatively high affinity for glucose (39) and is significantly upregulated when glucose becomes limiting (23). In nutrient-rich LB medium, glucose transport is inhibited, as *Pseudomonas* species prefer to use organic acids and amino acids as a carbon source instead (40, 41). A similar glucose-specific and OprB1-dependent cell lysis has been previously described for a *P.*

putida colR-deficient strain (23, 24). The lysis of the *colR* mutant was shown to result from the intolerance of the accumulation of OprB1 in the outer membrane, the cell's normal response to glucose limitation (23). Given that the TonB$_m$-PocAB-deficient strains have similar hypersensitivities to the OprB1 porin, we conclude that the outer membrane of the TonB$_m$-PocAB mutants is compromised. Furthermore, single-cell analysis revealed that, independent of the carbon source, the populations of TonB$_m$-PocAB mutants contain significantly more PI-permeable cells than the wild type (Fig. 2B). As propidium iodide can pass through undamaged outer membrane via porins but cannot cross intact cytoplasmic membrane (42), the increased permeability to PI implies that not only the outer membrane but also the inner membrane of the Δ*tonB$_m$* mutant is deficient.

The stress tolerance assays suggested that the fitness effects of TonB$_m$-PocAB's disruption were more pronounced when stationary-phase bacteria were analyzed (Fig. 3A and B). Considering that the growth characteristics of the Δ*tonB$_m$* strain also depended on the growth phase of the inoculum under unstressed conditions (Fig. 3C and D), the TonB$_m$-PocAB complex seems to be more important for stationary- than for exponential-phase bacteria. The proteome analysis provided a likely explanation for this growth phase dependence, namely, extensive differences, including upregulation of many metabolism-related stress response and regulatory proteins, were observed in the exponentially growing Δ*tonB$_m$* strain, while only a few proteomic changes were detected in the stationary-phase Δ*tonB$_m$* strain. This suggests that exponentially growing cells are actively dealing with the stress caused by the absence of functional TonB$_m$-PocAB, while stationary-phase cells lack this reprogramming, perhaps due to energy limitation, and cannot cope with the effects of TonB$_m$-PocAB deficiency. Thus, we assume that the ability of exponentially growing cells to compensate for the absence of the TonB$_m$-PocAB system allows them to preserve the wild-type-like growth rate in rich medium and start growth in the presence of stress.

Besides growth phase differences, the proteome data confirmed that the TonB$_m$-PocAB complex is necessary for maintaining membrane integrity. First, most of the proteins with changed expression in stationary-phase Δ*tonB$_m$* cells were membrane proteins that were upregulated in the wild-type but not in the Δ*tonB$_m$* strain. This hints that the cell envelope of the TonB$_m$-PocAB-deficient strain is sensitive to membrane protein upregulation, somewhat analogously to the sensitivity of OprB1 in glucose medium. Second, as the expression of 31 AlgU regulon proteins was found to be changed in the exponentially growing Δ*tonB$_m$* strain, AlgU seems to be activated in the Δ*tonB$_m$* strain. AlgU is an envelope stress response sigma factor that controls the expression of large numbers of genes (37). Under normal growth conditions, AlgU is bound to the anti-sigma factor MucA, which anchors it to the cytoplasmic membrane and prohibits it from regulating gene expression (43). Under cell envelope stress, induced either by cell wall-acting antibiotics or other compounds that disrupt bacterial membranes (37, 44) or by the overexpression of certain outer membrane proteins (43), MucA is degraded and AlgU is released into the cytoplasm (37). Therefore, the activation of the AlgU regulon indicates that the TonB$_m$-PocAB-deficient cells must experience envelope stress. Third, a large part of the differentially expressed proteins in exponentially growing Δ*tonB$_m$* strain (61 out of 126) overlapped the proteome response previously observed in *colR*-deficient *P. putida* treated with $ZnSO_4$ (26). This included many AlgU-regulated and stress-related proteins, the expression of which could be explained by the activation of AlgU in both strains, but also several other proteins, such as pyoverdine synthesis and type VI secretion system proteins. Analogously to AlgU regulon genes, the pyoverdine genes in *P. aeruginosa* are controlled by extracytoplasmic-function (ECF) sigma factors such as PvdS, FpvI, and SigX (45, 46). Given that activation of ECF sigma factors depends on transmembrane signaling, the upregulation of pyoverdine synthesis proteins may result from membrane stress as well. Since the Δ*tonB$_m$* strain and the *colR* mutant possess several common traits indicating their membrane deficiency, the overlapping proteome response can be considered an indicator of a similar type of envelope stress of the two mutants.

However, we should emphasize that compared to $TonB_m$-PocAB-deficient strains, the inactivation of ColRS signaling results in significantly milder phenotypes: *colR* mutant displays a lower level of glucose-dependent lysis and higher stress tolerance (except for metals like zinc, iron, and cadmium) and has no swimming deficiency (Fig. 9 and data not shown).

In addition to the AlgU regulon, the ColR regulon is activated in the Δ*tonB*$_m$ strain as well. This response most likely can somewhat alleviate the envelope stress, because the Δ*tonB*$_m$ *colR* double mutant displays a stronger growth defect (Fig. 3C and D) and has lower stress tolerance than the strain deficient only in *tonB*$_m$ (Fig. 9A and B). This suggests that the ColRS and $TonB_m$-PocAB systems have some overlap in their roles in membrane homeostasis. The activation of the ColR regulon in LB-growing Δ*tonB*$_m$ cells was somewhat surprising, particularly considering that ColS is a sensor that recognizes the excess of certain metals (25). However, there are two-component systems like PhoP/PhoQ that can sense different stimuli and also detect physical properties of the membrane (47–49). The current study suggests that, besides metals, ColS also senses membrane integrity and ColRS signaling can be triggered by membrane damage.

Both $TonB_m$-PocAB- and FlhF-deficient mutants have randomly placed flagella (Fig. 1B), but only $TonB_m$-PocAB deficiency results in membrane stress, indicating phenotypes like glucose-dependent lysis (Fig. 2A), increased membrane permeability (Fig. 2B), and lowered stress tolerance (Fig. 3). This shows that abnormal placement of flagella *per se* is not causing any membrane defects. Notably, in *P. aeruginosa*, the positioning of not only FlhF but also CheA, a chemotaxis histidine kinase with unipolar localization, becomes random in TonB3-PocAB-deficient strains (20), indicating that the TonB3-PocAB complex has a more general role in determining polar localization of different protein complexes. Interestingly, a somewhat similar role in the maintenance of membrane integrity as well as in the polar positioning of certain proteins has been reported for the Tol-Pal complex (50, 51). The transenvelope Tol-Pal complex consists of an outer membrane lipoprotein, Pal, a periplasmic protein, TolB, and inner membrane-situated TolA, TolQ, and TolR that are paralogous to $TonB_m$, PocA, and PocB, respectively. The Tol-Pal complex is part of the cell division machinery. It localizes to the division plane in early predivisional cells, assists proper invagination of the outer membrane, and remains at the new pole until division is completed (51, 52). Besides that, the Tol-Pal complex interacts with chemoreceptors and is required for maintaining the polar positioning of chemoreceptor clusters (50). It is proposed that the Tol-Pal complex physically restricts the departure of the chemoreceptor clusters from the poles after cell division. However, not all polarly localized proteins in *E. coli* require Tol-Pal for their maintenance in the pole (50). Given that the TonB3-PocAB complex itself is not polarly localized (20), the mechanism of how it determines the polar placement of FlhF and flagella should be indirect and likely does not resemble the mechanism described for the Tol-Pal complex. While the requirements for polar positioning of FlhF are not known, several characteristics of the cell pole can be considered. For example, it has been hypothesized that FlhF detects membrane curvature or recognizes specific proteins or lipids (e.g., cardiolipin and phosphatidylethanolamine) that are enriched at cell poles (53–56). It cannot be ruled out that the TonB-PocAB complex controls the polar placement of FlhF via a specific regulatory mechanism. Still, in light of the current results, we propose that the yet-undetermined polar marker for FlhF is altered due to the membrane defect of the $TonB_m$-PocAB mutant, which then results in the characteristic mislocalization of flagella.

TonB-like proteins connect the inner and outer membrane, as they are situated in the inner membrane and interact with outer membrane proteins. For instance, TonB of *E. coli* interacts with TonB-dependent outer membrane transporters to mediate siderophore uptake (12, 57). While it is reasonable to assume that the $TonB_m$-PocAB complex has a similar role in bridging the two membranes in *P. putida*, our attempts to detect the potential interaction partners of $TonB_m$ have been unsuccessful so far (data not shown). Hopefully, further studies will reveal the putative interaction partners of $TonB_m$

and disclose the true mechanism of how TonB$_m$-PocAB maintains membrane integrity and polar positioning of flagella.

MATERIALS AND METHODS

Bacterial strains, plasmids, and growth conditions. The bacterial strains and plasmids used are listed in Table 1. All strains are derivatives of *P. putida* PaW85 (58), which is isogenic to the fully sequenced KT2440 (59). Bacteria were grown in lysogeny broth (LB) or on minimal medium (60) containing 0.2% glucose. When selection was necessary, the growth medium was supplemented with benzylpenicillin (800 μg/ml), kanamycin (50 μg/ml), or streptomycin (200 μg/ml) for *P. putida* and kanamycin (50 μg/ml) or streptomycin (20 μg/ml) for *E. coli*. *E. coli* was incubated at 37°C and *P. putida* at 30°C. Bacteria were electrotransformed according to the protocol of Sharma and Schimke (61).

***P. putida* transposon mutant library screening for identification of Congo red binding mutants.** Wild-type *P. putida* was subjected to mutagenesis using a Tn*5*-based minitransposon, miniTn5Sm-lacItac. Plasmid pUTTn5Sm-lacItac was conjugatively transferred from the *E. coli* CC118 λ*pir* strain into *P. putida* PaW85 with the aid of the helper plasmid pRK2013. Transconjugants with random chromosomal insertions of the minitransposon were selected on 0.2% glucose minimal plates supplemented with streptomycin, Congo red (0.0005%), and 2 mM phenol. We searched for pink colonies among the white ones. Pink colonies were analyzed by arbitrary PCR and sequencing. PCR products were generated by two rounds of amplification as described elsewhere (62). In the first round, oligonucleotides prtac, specific for the *tac* promoter, and the arbitrary Arb6 were used as primers. Second-round PCR was performed with the primers OEint and Arb2. Screening of about 35,000 transposon mutants yielded five independent transposon insertions into the *tonB$_m$* gene and one into the *pocA* gene.

Construction of plasmids and strains. For the generation of deletion strains, the pEMG-based plasmids were constructed according to a protocol described elsewhere (63). The upstream and downstream regions (about 500 bp) of the gene(s) to be deleted were amplified separately and then joined into an approximately 1-kb fragment by overlap extension PCR. Oligonucleotides used in PCR amplifications are listed in Table 1. For construction of the plasmid pEMG/Δ*tonB$_m$*, the PCR fragment was cut with BamHI and EcoRI. For construction of the pEMG/Δ*pocA*, pEMG/Δ*pocB*, pEMG/Δ*pocAB*, pEMG/Δ*flhF*, and pEMG/Δ*mexCD-oprJ* plasmids, the PCR fragments were cut with XbaI and EcoRI. For construction of pEMG/Δ*nfxB*, EcoRI and SacI were used. The cut fragments were then ligated into the corresponding sites of the plasmid pEMG. The obtained pEMG plasmids were delivered to *P. putida* PaW85 or its deletion strains by electroporation, and after 2.5 h of growth in LB medium the bacteria were plated onto LB agar supplemented with kanamycin. Kanamycin-resistant cointegrates were selected and electrotransformed with the I-SceI expression plasmid pSW(I-SceI). To resolve the cointegrate, the plasmid-encoded I-SceI was induced with 1.5 mM 3-methylbenzoate overnight. Kanamycin-sensitive colonies were selected and the deletions were verified by PCR. The plasmid pSW(I-SceI) was eliminated from the deletion strains by growing them overnight in LB medium without antibiotics.

For complementation of the Δ*tonB$_m$* strain, the *tonB$_m$* gene amplified with the oligonucleotides 4994alg and 4994lopp was first cloned under the control of the *tac* promoter and *lacI*^{q} repressor in pBRlacItac. The *lacI*^{q}-P$_{tac}$-*tonB$_m$* cassette was excised from pBRlacItac/*tonB$_m$* with BamHI and subcloned into BamHI-opened pUCNotKm, resulting in pUCNotKm/*tactonB$_m$*. Finally, the TonB$_m$ expression cassette was inserted as a NotI fragment into the minitransposon delivery vector pBK-miniTn7-ΩSm. The obtained pminiTn7Sm/*tactonB$_m$* was introduced to the *E. coli* CC118 λ*pir* strain and conjugatively transformed into the *P. putida* Δ*tonB$_m$* strain with the help of pRK2013. The chromosomal presence of the *lacI*^{q}-P$_{tac}$-*tonB$_m$* cassette was verified by PCR.

For construction of C-terminal fluorescent fusion to FlhF, the *flhF* gene was PCR amplified using primers flhFEco and flhFXho. The EcoRI-XhoI-cleaved *flhF* fragment was then used to replace the *colR* gene in the *colR-gfp* translational fusion in plasmid pKTlacItac/*colR-gfp* (laboratory collection). The *lacI*^{q}-P$_{tac}$-*flhF-gfp* cassette then was inserted into SmaI-KpnI-opened miniTn*7* delivery plasmid pGP-miniTn*7*-ΩGm. The plasmid pGPminiTn7Gm/lacItac-*flhF-gfp* was introduced into the *P. putida* wild-type, Δ*tonB$_m$*, Δ*flhF*, and Δ*tonB$_m$* Δ*flhF* strains by coelectroporation together with the helper plasmid pUXBF13. The presence of the *lacI*^{q}-P$_{tac}$-*flhF-gfp* cassette in the *att*Tn*7* site was verified by PCR.

For construction of *oprB1*-deficient strains, p704L/oprB1::Sm plasmid was introduced into the *E. coli* CC118 λ*pir* strain and conjugatively transformed into *P. putida* Δ*tonB$_m$*, Δ*pocA*, Δ*pocB*, and Δ*tonB$_m$* Δ*flhF* strains with the help of pRK2013 (64). *oprB1* deficiency was verified by PCR.

Motility assay. The motility assay was conducted on petri dishes containing 20 ml of LB medium supplemented with 0.3% agarose. Motility was assessed by inoculating 1 μl of overnight culture into the medium and measuring the diameter of growth after incubating the petri dishes at 30°C for 18 h.

Microscopy analysis of flagellum localization. Bacteria were grown in 5 ml LB medium at 30°C until the optical density at 580 nm (OD$_{580}$) was ~1. The cells were centrifuged at 1,700 × *g* for 45 s, washed twice with distilled water, and gently resuspended in 1 ml distilled water. Ten-microliter drops of bacterial dilutions (100 cells/μl) were slowly dried on a microscopy slide. The dried drops were covered with stain [0.31% $FeCl_3$, 6.25% tannin, 92 mM $AlK(SO_4)_2$] for 4 min, washed with distilled water, and allowed to dry again. The dried drops were then covered with 5% $AgNO_3$ and 0.0125% NH_4OH solution for 3 min, washed with distilled water, and allowed to dry. Bacteria were observed using oil immersion light microscopy (×1,000 magnification).

Congo red binding assay. Bacteria were grown overnight in 5 ml LB and diluted 100-fold, and 5-μl drops were inoculated onto glucose minimal medium plate containing 0.0005% Congo red dye. The plate was incubated at 30°C for 72 h.

TABLE 1 Strains and plasmids

Strain or plasmid	Genotype or characteristics	Source or reference
Strains		
Escherichia coli CC118 λ*pir*	Δ(*ara-leu*) *araD* Δ*lacX74 galE galK phoA20 thi-1 rpsE rpoB argE*(Am) *recA1* λ*pir* lysogen	73
Pseudomonas putida		
PaW85	Wild type, isogenic to KT2440	58
colR strain	PaW85 *colR*::Km (Km^r)	74
Δ$tonB_m$ strain	PaW85 ΔPP_4994	This study
Δ*pocA* strain	PaW85 ΔPP_1898	This study
Δ*pocB* strain	PaW85 ΔPP_1899	This study
Δ$tonB_m$ Δ*pocAB* strain	PaW85 ΔPP_4994 ΔPP_1898-PP_1898	This study
Δ*flhF* strain	PaW85 ΔPP_4343	This study
Δ$tonB_m$ Δ*flhF* strain	Δ$tonB_m$ Δ*flhF*	This study
Δ$tonB_m$ *tac-tonB$_m$* strain	Δ$tonB_m$ with genomic *lacI^q-P$_{tac}$-tonB$_m$* expression cassette (Sm^r)	This study
wt/*flhF-gfp* strain	Wild type with genomic *lacI^q-P$_{tac}$-flhF-gfp* expression cassette (Gm^r)	This study
Δ$tonB_m$/*flhF-gfp* strain	Δ$tonB_m$ with genomic *lacI^q-P$_{tac}$-flhF-gfp* expression cassette (Gm^r)	This study
Δ*flhF/flhF-gfp* strain	Δ*flhF* with genomic *lacI^q-P$_{tac}$-flhF-gfp* expression cassette (Gm^r)	This study
Δ$tonB_m$ Δ*flhF/flhF-gfp* strain	Δ$tonB_m$ Δ*flhF* with genomic *lacI^q-P$_{tac}$-flhF-gfp* cassette (Gm^r)	This study
Δ$tonB_m$ *oprB1* strain	Δ$tonB_m$ and PP_1019::Sm (Sm^r)	This study
Δ*pocA oprB1* strain	Δ*pocA* and PP_1019::Sm (Sm^r)	This study
Δ*pocB oprB1* strain	Δ*pocB* and PP_1019::Sm (Sm^r)	This study
Δ$tonB_m$ Δ*flhF-oprB1* strain	Δ$tonB_m$ Δ*flhF* PP_1019::Sm (Sm^r)	This study
Δ*mexCD-oprJ* strain	PaW85 ΔPP_2817-2819	This study
Δ$tonB_m$ Δ*mexCD-oprJ* strain	Δ$tonB_m$ ΔPP_2817-2819	This study
Δ*nfxB* strain	PaW85 ΔPP_2820	This study
Δ$tonB_m$ Δ*nfxB* strain	Δ$tonB_m$ ΔPP_2820	This study
Δ$tonB_m$ *colR* strain	Δ$tonB_m$*colR*::Km (Km^r)	This study
Plasmids		
pUTTn5Sm-lacItac	Delivery plasmid for miniTn*5*Sm-lacItac (Ap^r Sm^r)	75
pRK2013	Helper plasmid for conjugal transfer (Km^r)	64
pKTlacZS/C	Transcriptional fusion of Tn*4652 tnpA* with *lacZ* in pKTlacZ	76
pEMG	Plasmid for homologous recombination, *lacZa* with two flanking I-SceI sites (Km^r)	63
pEMG/Δ$tonB_m$	pEMG containing chimeric DNA fragment for deleting PP_4994 (Km^r)	This study
pEMG/Δ*pocA*	pEMG containing chimeric DNA fragment for deleting PP_1898 (Km^r)	This study
pEMG/Δ*pocB*	pEMG containing chimeric DNA fragment for deleting PP_1899 (Km^r)	This study
pEMG/Δ*pocAB*	pEMG containing chimeric DNA fragment for deleting PP_1898 and PP_1899 (Km^r)	This study
pEMG/Δ*flhF*	pEMG containing chimeric DNA fragment for deleting PP_4343 (Km^r)	This study
pEMG/Δ*mexCD-oprJ*	pEMG containing chimeric DNA fragment for deleting ΔPP_2817-2819 operon (Km^r)	This study
pEMG/Δ*nfxB*	pEMG containing chimeric DNA fragment for deleting PP_2820 (Km^r)	This study
pSW (I-SceI)	Plasmid coding for I-SceI endonuclease for allelic exchange experiments (Bp^r)	77
p704L/*oprB1*::Sm	pGP704L with EcoRI fragment of *oprB1*::Sm from pKS/*oprB1*::Sm (Ap^r Sm^r)	78
pBRlacItac	Expression vector containing *lacI^q* repressor-controlled P$_{tac}$ promoter (Amp^r)	79
pBRlacItac/*tonB$_m$*	pBRlacItac containing *tonB$_m$* in a 1,044-bp HindIII-XbaI fragment under the *P$_{tac}$* promoter (Amp^r)	This study
pUCNotKm	Cloning vector (Km^r)	80
pUCNotKm/*tactonB$_m$*	pUCNot containing *lacI^q-P$_{tac}$-tonB$_m$* expression cassette (Amp^r)	This study
pBK-miniTn*7*-ΩSm	pUC19-based delivery plasmid for miniTn*7*-ΩSm (Amp^r Sm^r)	81
pminiTn*7*tac-*tonB$_m$*	pBK-miniTn*7*-ΩSm containing *lacI^q-P$_{tac}$-tonB$_m$* expression cassette (Amp^r Sm^r)	This study
pKTlacItac	Expression vector	82
pKTlacItac/*flhF-gfp*	Plasmid for expression of FlhF-GFP fusion protein (Amp^r)	This study
pGP-mini-Tn*7*-ΩGm	Delivery plasmid for mini-Tn*7*-ΩGm (Amp^r Gm^r)	83
pGPminiTn*7*Gm/*lacItac-flhF-gfp*	Delivery plasmid for miniTn*7*Gm-*lacItac-flhF-gfp* (Amp^r Gm^r)	This study
pUXBF13	Plasmid coding for the Tn*7* transposition proteins (Amp^r, *mob*$^+$)	84
p9TT$_B$lacZ/*algD*	PP_1288 promoter fused with *lacZ* in p9TT$_B$lacZ (Amp^r Cm^r)	78
p9TT$_B$lacZ/*amrZ*	PP_4470 promoter fused with *lacZ* in p9TT$_B$lacZ (Amp^r Cm^r)	26
p9TT$_B$lacZ/*oprQ*	PP_0268 promoter fused with *lacZ* in p9TT$_B$lacZ (Amp^r Cm^r)	78
p9TT$_B$lacZ/*903*	PP_0903 promoter fused with *lacZ* in p9TT$_B$lacZ (Amp^r Cm^r)	38
p9TT$_B$lacZ/*5152*	PP_5152 promoter fused with *lacZ* in p9TT$_B$lacZ (Amp^r Cm^r)	25
p9TT$_B$lacZ/*900*	PP_0900 promoter fused with *lacZ* in p9TT$_B$lacZ (Amp^r Cm^r)	38

β-Galactosidase leakage assay. Strains containing the pKTlacZS/C plasmid were grown on solid glucose minimal or LB medium at 30°C for 20 h. Cells were suspended in 500 μl M9 buffer and centrifuged for 1 min at 12,000 × *g*, and the supernatant was used to measure β-galactosidase activity according to a previously described protocol (65).

Flow cytometry analysis. Bacteria were grown overnight in 5 ml LB and diluted 100-fold, and 5-μl drops were inoculated onto agar plates with glucose minimal medium or LB. After 24 h of growth at 30°C,

the cells were scraped off from the plates and suspended in 1 ml M9 buffer. The optical density of the cell suspension was diluted to an OD_{580} of 0.015. The two components of the LIVE/DEAD BacLight kit (L7012; Invitrogen), 20 mM red fluorescent dye propidium iodide (PI) and 3.34 mM green fluorescent dye SYTO9, were mixed at a 1:1 volume ratio and then diluted 17.6-fold into filter-sterilized M9 buffer. For staining of bacteria, the diluted cell suspension was mixed with the freshly prepared reagent mixture at a 20:1 ratio. Samples were incubated at 30°C in the dark for 30 min, and approximately 10,000 events from every sample were analyzed with a FACSAria flow cytometer (BD Biosciences). Fluorescent dyes were excited at 488 nm. Forward and side scatter of the light and fluorescence emission at 530 and 616 nm were acquired for every event. Populations of intact, PI-permeable, and dead cells were defined as previously described (28). While PI-permeable cells differ from the intact subpopulation only by their PI-permeable membrane, the dead cells are more compromised, containing less DNA than other cells (28).

Stress tolerance plate assay. To evaluate the stress tolerance, bacteria were grown overnight (stationary phase) or to an OD_{580} of ~1 (exponential phase) in 5 ml LB medium. Serial dilutions were spotted as 5-μl drops onto LB agar plates supplemented with different chemicals (specified in Results). Plates were incubated at 30°C for 20 h.

Growth curve and minimal generation time. To start the assay always with cells in the same physiological state, 50-μl stocks made of overnight-grown bacteria were used. To investigate the growth curve of bacteria starting from stationary phase, cells were inoculated from stock into 5 ml LB medium and grown for 21 h (OD_{580} of ~4) at 30°C. For exponential-phase cells, 100 μl of the bacteria grown for 18 h were diluted into fresh LB medium and grown for 3 h (OD_{580} of ~1) at 30°C. The optical densities of microbial cultures at 580 nm were measured and the bacteria were diluted in LB medium for the OD_{580} to be 0.1. Aliquots of 100 μl of the dilutions were transferred into microtiter plate wells, and the cells were grown at 30°C and 400 rpm inside a POLARstar Omega plate reader spectrophotometer. The OD_{580} was measured every 7 min. Data were collected with the Omega data analysis software.

Minimal generation time was calculated from the slope of the most rapid exponential growth according to the formula $G = t/3.3\log(b/B)$, where G marks the generation time, t is the time interval in minutes, and B and b are OD_{580} at the beginning and the end of the time interval, respectively.

Isolation of outer membrane proteins. For the isolation of OMPs of stationary-phase cells, bacteria were grown in 30 ml LB medium at 30°C for 17 h. To obtain the OMPs of exponentially growing cells, bacteria were grown in 200 ml LB for 3 h at 30°C to an OD_{580} of 0.9. Cells were collected by centrifugation at 5,000 × *g* at 4°C for 10 min, washed with 6 ml of 10 mM HEPES buffer (pH 7.4), and resuspended in 3 ml of the same buffer. Cells were then disrupted by ultrasonication, and cell debris was pelleted by centrifugation at 7,000 × *g* at 4°C for 15 min. Further OMP isolation was done as described previously (23). One-microgram samples of isolated OMPs were loaded onto 10% SDS-PAGE gel and stained according to a previous protocol (66).

Label-free proteomic analysis. (i) Growth conditions and nano-LC-MS/MS analysis. Bacteria were pregrown overnight in liquid LB at 30°C, diluted into fresh LB medium (OD_{580} of ~0.1), and grown either up to an OD_{580} of ~1 (exponential phase) or for 17 h (stationary phase). Cells were harvested at 5,000 × *g* at 4°C for 10 min, resuspended in lysis buffer (4% SDS, 100 mM Tris, pH 7.5, 10 mM dithiothreitol), heated at 95°C for 5 min, and sonicated. The protein concentration was measured by tryptophan fluorescence, and 30 μg of cellular protein was loaded onto 30-kDa-cutoff Vivacon 500 ultrafiltration spin columns (Sartorius). Three independent samples of exponential- and stationary-phase *P. putida* wild-type and Δ*tonB$_m$* cells were digested for 4 h on filter with 1:50 Lys-C (Wako) and then overnight with 1:50 proteomics-grade dimethylated trypsin (Sigma-Aldrich) as described for the filter-aided sample preparation protocol (67). Peptides were desalted with C_{18} StageTips (68), eluted, dried, and reconstituted in 0.5% trifluoroacetic acid. Nano-liquid chromatography-tandem mass spectrometry (LC-MS/MS) analysis was performed as described previously (69) using an Ultimate 3000 RSLCnano system (Dionex) and a Q Exactive mass spectrometer (Thermo Fisher Scientific) operating with top-10 data-dependent acquisition.

(ii) MS raw data processing. Raw data were identified and quantified with the MaxQuant 1.4.0.8 software package (70). Label-free quantification with MaxQuant LFQ algorithm (71) was enabled with default settings. Methionine oxidation and protein N-terminal acetylation were set as variable modifications, while cysteine carbamidomethylation was defined as a fixed modification. A search was performed against the UniProt (www.uniprot.org) *P. putida* KT2440 database (April 2015 version) using the tryptic digestion rule (cleavage after lysine and arginine without proline restriction). Identifications with minimally one peptide of at least seven amino acids were accepted, and transfer of identifications between runs was enabled. Protein quantification criteria were set to two peptides with a minimum of two consecutive MS1 scans per peptide. Peptide-spectrum match and protein false discovery rate were kept below 1% using a target-decoy approach. All other parameters were kept at default.

(iii) Quantitative protein profiling. Data analysis was performed with the Perseus software (72). The whole data set contained 3,359 different proteins. Parallel samples were grouped together, and groups were compared in pairs: (i) *P. putida* wild type from exponential (wt^E) versus stationary (wt^S) phase (2,652 proteins), (ii) Δ*tonB$_m$* strain from exponential ($tonB^E$) versus stationary ($tonB^S$) phase (2,673 proteins), (iii) wt^E versus $tonB^E$ (2,406 proteins), and (iv) wt^S versus $tonB^S$ (2,556 proteins). To be included in the analysis, a protein needed to be detected in all three parallels of one group. Thereafter, missing values were imputed using default settings. Mean protein abundances were compared between two groups using the independent-sample Student *t* test. The Benjamini-Hochberg multiple-testing correction was applied with the false discovery rate set to 0.05.

SUPPLEMENTAL MATERIAL

Supplemental material for this article may be found at https://doi.org/10.1128/JB.00303-19.

SUPPLEMENTAL FILE 1, XLSX file, 1.1 MB.

SUPPLEMENTAL FILE 2, PDF file, 0.5 MB.

ACKNOWLEDGMENTS

We thank Sirli Rosendahl and Andres Ainelo for critical reading of the manuscript and Dmitri Lubenets for technical assistance.

This work was supported by the Estonian Research Council grants IUT20-19, IUT2-22, and PUT1351.

REFERENCES

1. Silhavy TJ, Kahne D, Walker S. 2010. The bacterial cell envelope. CSH Perspect Biol 2:a000414. https://doi.org/10.1101/cshperspect.a000414.
2. Postle K, Larsen RA. 2007. TonB-dependent energy transduction between outer and cytoplasmic membranes. Biometals 20:453–465. https://doi.org/10.1007/s10534-006-9071-6.
3. Wiener MC, Horanyi PS. 2011. How hydrophobic molecules traverse the outer membranes of Gram-negative bacteria. Proc Natl Acad Sci U S A 108:10929–10930. https://doi.org/10.1073/pnas.1106927108.
4. Schauer K, Rodionov DA, de Reuse H. 2008. New substrates for TonB-dependent transport: do we only see the"tip of the iceberg"? Trends Biochem Sci 33:330–338. https://doi.org/10.1016/j.tibs.2008.04.012.
5. Celia H, Noinaj N, Zakharov SD, Bordignon E, Botos I, Santamaria M, Barnard TJ, Cramer WA, Lloubes R, Buchanan SK. 2016. Structural insight into the role of the Ton complex in energy transduction. Nature 538:60. https://doi.org/10.1038/nature19757.
6. Baker KR, Postle K. 2013. Mutations in *Escherichia coli* ExbB transmembrane domains identify scaffolding and signal transduction functions and exclude participation in a proton pathway. J Bacteriol 195:2898–2911. https://doi.org/10.1128/JB.00017-13.
7. Maki-Yonekura S, Matsuoka R, Yamashita Y, Shimizu H, Tanaka M, Iwabuki F, Yonekura K. 2018. Hexameric and pentameric complexes of the ExbBD energizer in the Ton system. Elife 7:e35419. https://doi.org/10.7554/eLife.35419.
8. Ollis AA, Postle K. 2012. ExbD mutants define initial stages in TonB energization. J Mol Biol 415:237–247. https://doi.org/10.1016/j.jmb.2011.11.005.
9. Gresock MG, Kastead KA, Postle K. 2015. From homodimer to heterodimer and back: elucidating the TonB energy transduction cycle. J Bacteriol 197:3433–3445. https://doi.org/10.1128/JB.00484-15.
10. Ollis AA, Kumar A, Postle K. 2012. The ExbD periplasmic domain contains distinct functional regions for two stages in TonB energization. J Bacteriol 194:3069–3077. https://doi.org/10.1128/JB.00015-12.
11. Skare JT, Ahmer BMM, Seachord CL, Darveau RP, Postle K. 1993. Energy transduction between membranes–TonB, a cytoplasmic membrane protein, can be chemically cross-linked in-vivo to the outer membrane receptor FepA. J Biol Chem 268:16302–16308.
12. Ogierman M, Braun V. 2003. Interactions between the outer membrane ferric citrate transporter FecA and TonB: studies of the FecA TonB box. J Bacteriol 185:1870–1885. https://doi.org/10.1128/JB.185.6.1870-1885.2003.
13. Cafiso DS. 2014. Identifying and quantitating conformational exchange in membrane proteins using site-directed spin labeling. Acc Chem Res 47:3102–3109. https://doi.org/10.1021/ar500228s.
14. Chu BCH, Peacock RS, Vogel HJ. 2007. Bioinformatic analysis of the TonB protein family. Biometals 20:467–483. https://doi.org/10.1007/s10534-006-9049-4.
15. Bitter W, Tommassen J, Weisbeek PJ. 1993. Identification and characterization of the *exbB*, *exbD* and *tonB* genes of *Pseudomonas putida* WCS358: their involvement in ferric-pseudobactin transport. Mol Microbiol 7:117–130. https://doi.org/10.1111/j.1365-2958.1993.tb01103.x.
16. Godoy P, Ramos-Gonzalez MI, Ramos JL. 2004. *Pseudomonas putida* mutants in the *exbBexbDtonB* gene cluster are hypersensitive to environmental and chemical stressors. Environ Microbiol 6:605–610. https://doi.org/10.1111/j.1462-2920.2004.00595.x.
17. Godoy P, Ramos-Gonzalez MI, Ramos JL. 2001. Involvement of the TonB system in tolerance to solvents and drugs in *Pseudomonas putida* DOT-T1E. J Bacteriol 183:5285–5292. https://doi.org/10.1128/JB.183.18.5285-5292.2001.
18. Molina MA, Godoy P, Ramos-Gonzalez MI, Munoz N, Ramos JL, Espinosa-Urgel M. 2005. Role of iron and the TonB system in colonization of corn seeds and roots by *Pseudomonas putida* KT2440. Environ Microbiol 7:443–449. https://doi.org/10.1111/j.1462-2920.2005.00720.x.
19. Winsor GL, Griffiths EJ, Lo R, Dhillon BK, Shay JA, Brinkman F. 2016. Enhanced annotations and features for comparing thousands of Pseudomonas genomes in the Pseudomonas genome database. Nucleic Acids Res 44:D646–D653. https://doi.org/10.1093/nar/gkv1227.
20. Cowles KN, Moser TS, Siryaporn A, Nyakudarika N, Dixon W, Turner JJ, Gitai Z. 2013. The putative Poc complex controls two distinct *Pseudomonas aeruginosa* polar motility mechanisms. Mol Microbiol 90:923–938. https://doi.org/10.1111/mmi.12403.
21. Shirley M, Lamont IL. 2009. Role of TonB1 in pyoverdine-mediated signaling in *Pseudomonas aeruginosa*. J Bacteriol 191:5634–5640. https://doi.org/10.1128/JB.00742-09.
22. Huang BX, Ru K, Yuan Z, Whitchurch CB, Mattick JS. 2004. *tonB3* is required for normal twitching motility and extracellular assembly of type IV pili. J Bacteriol 186:4387–4389. https://doi.org/10.1128/JB.186.13.4387-4389.2004.
23. Putrinš M, Ainelo A, Ilves H, Hõrak R. 2011. The ColRS system is essential for the hunger response of glucose-growing *Pseudomonas putida*. BMC Microbiol 11:170. https://doi.org/10.1186/1471-2180-11-170.
24. Putrinš M, Ilves H, Kivisaar M, Hõrak R. 2008. ColRS two-component system prevents lysis of subpopulation of glucose-grown *Pseudomonas putida*. Environ Microbiol 10:2886–2893. https://doi.org/10.1111/j.1462-2920.2008.01705.x.
25. Ainsaar K, Mumm K, Ilves H, Hõrak R. 2014. The ColRS signal transduction system responds to the excess of external zinc, iron, manganese, and cadmium. BMC Microbiol 14:162. https://doi.org/10.1186/1471-2180-14-162.
26. Mumm K, Ainsaar K, Kasvandik S, Tenson T, Hõrak R. 2016. Responses of *Pseudomonas putida* to zinc excess determined at the proteome level: pathways dependent and independent of ColRS. J Proteome Res 15:4349–4368. https://doi.org/10.1021/acs.jproteome.6b00420.
27. Pandza S, Baetens M, Park CH, Au T, Keyhan M, Matin A. 2000. The G-protein FlhF has a role in polar flagellar placement and general stress response induction in Pseudomonas putida. Mol Microbiol 36:414–423. https://doi.org/10.1046/j.1365-2958.2000.01859.x.
28. Putrinš M, Ilves H, Lilje L, Kivisaar M, Hõrak R. 2010. The impact of ColRS two-component system and TtgABC efflux pump on phenol tolerance of *Pseudomonas putida* becomes evident only in growing bacteria. BMC Microbiol 10:110. https://doi.org/10.1186/1471-2180-10-110.
29. Masuda N, Sakagawa E, Ohya S, Gotoh N, Tsujimoto H, Nishino T. 2000. Substrate specificities of MexAB-OprM, MexCD-OprJ, and MexXY-OprM efflux pumps in *Pseudomonas aeruginosa*. Antimicrob Agents Chemother 44:3322–3327. https://doi.org/10.1128/AAC.44.12.3322-3327.2000.
30. Olivera ER, Minambres B, Garcia B, Muniz C, Moreno MA, Ferrandez A, Diaz E, Garcia JL, Luengo JM. 1998. Molecular characterization of the phenylacetic acid catabolic pathway in *Pseudomonas putida* U: the phenylacetyl-CoA catabolon. Proc Natl Acad Sci U S A 95:6419–6424. https://doi.org/10.1073/pnas.95.11.6419.
31. Purssell A, Poole K. 2013. Functional characterization of the NfxB repressor of the *mexCD-oprJ* multidrug efflux operon of *Pseudomonas aeruginosa*. Microbiology 159:2058–2073. https://doi.org/10.1099/mic.0.069286-0.

32. Purssell A, Fruci M, Mikalauskas A, Gilmour C, Poole K. 2015. EsrC, an envelope stress-regulated repressor of the mexCD-oprJ multidrug efflux operon in *Pseudomonas aeruginosa*. Environ Microbiol 17:186–198. https://doi.org/10.1111/1462-2920.12602.
33. Poole K, Gotoh N, Tsujimoto H, Zhao QX, Wada A, Yamasaki T, Neshat S, Yamagishi JI, Li XZ, Nishino T. 1996. Overexpression of the *mexC-mexD-oprJ* efflux operon in *nfxB*-type multidrug-resistant strains of *Pseudomonas aeruginosa*. Mol Microbiol 21:713–724. https://doi.org/10.1046/j.1365-2958.1996.281397.x.
34. Jeannot K, Elsen S, Köhler T, Attree I, van Delden C, Plesiat P. 2008. Resistance and virulence of *Pseudomonas aeruginosa* clinical strains overproducing the MexCD-OprJ efflux pump. Antimicrob Agents Chemother 52:2455–2462. https://doi.org/10.1128/AAC.01107-07.
35. Bernal P, Allsopp LP, Filloux A, Llamas MA. 2017. The *Pseudomonas putida* T6SS is a plant warden against phytopathogens. ISME J 11:972–987. https://doi.org/10.1038/ismej.2016.169.
36. Chang WS, van de Mortel M, Nielsen L, de Guzman GN, Li XH, Halverson LJ. 2007. Alginate production by *Pseudomonas putida* creates a hydrated microenvironment and contributes to biofilm architecture and stress tolerance under water-limiting conditions. J Bacteriol 189:8290–8299. https://doi.org/10.1128/JB.00727-07.
37. Wood LF, Ohman DE. 2009. Use of cell wall stress to characterize sigma(22) (AlgT/U) activation by regulated proteolysis and its regulon in *Pseudomonas aeruginosa*. Mol Microbiol 72:183–201. https://doi.org/10.1111/j.1365-2958.2009.06635.x.
38. Kivistik PA, Kivi R, Kivisaar M, Hõrak R. 2009. Identification of CoIR binding consensus and prediction of regulon of CoIRS two-component system. BMC Mol Biol 10:46. https://doi.org/10.1186/1471-2199-10-46.
39. Wylie JL, Worobec EA. 1995. The OprB porin plays a central role in carbohydrate uptake in *Pseudomonas aeruginosa*. J Bacteriol 177:3021–3026. https://doi.org/10.1128/jb.177.11.3021-3026.1995.
40. Moreno R, Martinez-Gomariz M, Yuste L, Gil C, Rojo F. 2009. The *Pseudomonas putida* Crc global regulator controls the hierarchical assimilation of amino acids in a complete medium: evidence from proteomic and genomic analyses. Proteomics 9:2910–2928. https://doi.org/10.1002/pmic.200800918.
41. Rojo F. 2010. Carbon catabolite repression in *Pseudomonas*: optimizing metabolic versatility and interactions with the environment. FEMS Microbiol Rev 34:658–684. https://doi.org/10.1111/j.1574-6976.2010.00218.x.
42. Gh MS, Wilhelm MJ, Sheffield JB, Dai HL. 2015. Living *E. coli* is permeable to propidium iodide: a study by time-resolved second-harmonic scattering and fluorescence microscopy. Biophys J 108:148A–149A. https://doi.org/10.1016/j.bpj.2014.11.819.
43. Qiu DR, Eisinger VM, Rowen DW, Yu H. 2007. Regulated proteolysis controls mucoid conversion in *Pseudomonas aeruginosa*. Proc Natl Acad Sci U S A 104:8107–8112. https://doi.org/10.1073/pnas.0702660104.
44. Wood LF, Leech AJ, Ohman DE. 2006. Cell wall inhibitory antibiotics activate the alginate biosynthesis operon in *Pseudomonas aeruginosa*: roles of sigma(22) (AlgT) and the AlgW and Prc proteases. Mol Microbiol 62:412–426. https://doi.org/10.1111/j.1365-2958.2006.05390.x.
45. Chevalier S, Bouffartigues E, Bazire A, Tahrioui A, Duchesne R, Tortuel D, Maillot O, Clamens T, Orange N, Feuilloley MGJ. 2018. Extracytoplasmic function sigma factors in *Pseudomonas aeruginosa*. Biochim Biophys Acta Gene Regul Mech 1862:706–721. https://doi.org/10.1016/j.bbagrm.2018.04.008.
46. Llamas MA, Imperi F, Visca P, Lamont IL. 2014. Cell-surface signaling in Pseudomonas: stress responses, iron transport, and pathogenicity. FEMS Microbiol Rev 38:569–597. https://doi.org/10.1111/1574-6976.12078.
47. Vescovi EG, Soncini FC, Groisman EA. 1996. Mg^{2+} as an extracellular signal: environmental regulation of *Salmonella* virulence. Cell 84:165–174. https://doi.org/10.1016/S0092-8674(00)81003-X.
48. Bader MW, Sanowar S, Daley ME, Schneider AR, Cho US, Xu WQ, Klevit RE, Le Moual H, Miller S. 2005. Recognition of antimicrobial peptides by a bacterial sensor kinase. Cell 122:461–472. https://doi.org/10.1016/j.cell.2005.05.030.
49. Yuan J, Jin F, Glatter T, Sourjik V. 2017. Osmosensing by the bacterial PhoQ/PhoP two-component system. Proc Natl Acad Sci U S A 114:E10792–E10798. https://doi.org/10.1073/pnas.1717272114.
50. Santos TMA, Lin TY, Rajendran M, Anderson SM, Weibel DB. 2014. Polar localization of *Escherichia coli* chemoreceptors requires an intact Tol-Pal complex. Mol Microbiol 92:985–1004. https://doi.org/10.1111/mmi.12609.
51. Yeh YC, Comolli LR, Downing KH, Shapiro L, McAdams HH. 2010. The *Caulobacter* Tol-Pal complex is essential for outer membrane integrity and the positioning of a polar localization factor. J Bacteriol 192:4847–4858. https://doi.org/10.1128/JB.00607-10.
52. Gerding MA, Ogata Y, Pecora ND, Niki H, de Boer P. 2007. The trans-envelope Tol-Pal complex is part of the cell division machinery and required for proper outer membrane invagination during cell constriction in *E. coli*. Mol Microbiol 63:1008–1025. https://doi.org/10.1111/j.1365-2958.2006.05571.x.
53. Gao T, Shi MM, Ju LL, Gao HC. 2015. Investigation into FlhFG reveals distinct features of FlhF in regulating flagellum polarity in *Shewanella oneidensis*. Mol Microbiol 98:571–585. https://doi.org/10.1111/mmi.13141.
54. Green JCD, Kahramanoglou C, Rahman A, Pender AMC, Charbonnel N, Fraser GM. 2009. Recruitment of the earliest component of the bacterial flagellum to the old cell division pole by a membrane-associated signal recognition particle family GTP-binding protein. J Mol Biol 391:679–690. https://doi.org/10.1016/j.jmb.2009.05.075.
55. Kondo S, Imura Y, Mizuno A, Homma M, Kojima S. 2018. Biochemical analysis of GTPase FlhF which controls the number and position of flagellar formation in marine Vibrio. Sci Rep 8:12115. https://doi.org/10.1038/s41598-018-30531-5.
56. Kusumoto A, Shinohara A, Terashima H, Kojima S, Yakushi T, Homma M. 2008. Collaboration of FlhF and FlhG to regulate polar-flagella number and localization in *Vibrio alginolyticus*. Microbiology 154:1390–1399. https://doi.org/10.1099/mic.0.2007/012641-0.
57. Higgs PI, Larsen RA, Postle K. 2002. Quantification of known components of the *Escherichia coli* TonB energy transduction system: TonB, ExbB, ExbD and FepA. Mol Microbiol 44:271–281. https://doi.org/10.1046/j.1365-2958.2002.02880.x.
58. Bayley SA, Duggleby CJ, Worsey MJ, Williams PA, Hardy KG, Broda P. 1977. Two modes of loss of the Tol function from *Pseudomonas putida* mt-2. Mol Gen Genet 154:203–204. https://doi.org/10.1007/BF00330838.
59. Regenhardt D, Heuer H, Heim S, Fernandez DU, Strompl C, Moore ERB, Timmis KN. 2002. Pedigree and taxonomic credentials of *Pseudomonas putida* strain KT2440. Environ Microbiol 4:912–915. https://doi.org/10.1046/j.1462-2920.2002.00368.x.
60. Adams MH. 1959. Bacteriophages. Interscience Publishers Inc., New York, NY.
61. Sharma RC, Schimke RT. 1996. Preparation of electro-competent *E. coli* using salt-free growth medium. Biotechniques 20:42–44. https://doi.org/10.2144/96201bm08.
62. O'Toole GA, Kolter R. 1998. Initiation of biofilm formation in *Pseudomonas fluorescens* WCS365 proceeds via multiple, convergent signalling pathways: a genetic analysis. Mol Microbiol 28:449–461. https://doi.org/10.1046/j.1365-2958.1998.00797.x.
63. Martinez-Garcia E, de Lorenzo V. 2011. Engineering multiple genomic deletions in Gram-negative bacteria: analysis of the multi-resistant antibiotic profile of *Pseudomonas putida* KT2440. Environ Microbiol 13:2702–2716. https://doi.org/10.1111/j.1462-2920.2011.02538.x.
64. Figurski DH, Helinski DR. 1979. Replication of an origin-containing derivative of plasmid RK2 dependent on a plasmid function provided in *trans*. Proc Natl Acad Sci U S A 76:1648–1652. https://doi.org/10.1073/pnas.76.4.1648.
65. Miller JH. 1992. A short course in bacterial genetics: a laboratory manual and handbook for Escherichia coli and related bacteria. Cold Spring Harbor Laboratory Press, New York, NY.
66. Chevallet M, Luche S, Rabilloud T. 2006. Silver staining of proteins in polyacrylamide gels. Nat Protoc 1:1852–1858. https://doi.org/10.1038/nprot.2006.288.
67. Wisniewski JR, Zougman A, Nagaraj N, Mann M. 2009. Universal sample preparation method for proteome analysis. Nat Methods 6:359–362. https://doi.org/10.1038/nmeth.1322.
68. Rappsilber J, Mann M, Ishihama Y. 2007. Protocol for micro-purification, enrichment, pre-fractionation and storage of peptides for proteomics using StageTips. Nat Protoc 2:1896–1906. https://doi.org/10.1038/nprot.2007.261.
69. Kasvandik S, Samuel K, Peters M, Eimre M, Peet N, Roost AM, Padrik L, Paju K, Peil L, Salumets A. 2016. Deep quantitative proteomics reveals extensive metabolic reprogramming and cancer-like changes of ectopic endometriotic stromal cells. J Proteome Res 15:572–584. https://doi.org/10.1021/acs.jproteome.5b00965.
70. Cox J, Mann M. 2008. MaxQuant enables high peptide identification rates, individualized p.p.b.-range mass accuracies and proteome-wide protein quantification. Nat Biotechnol 26:1367–1372. https://doi.org/10.1038/nbt.1511.
71. Cox J, Hein MY, Luber CA, Paron I, Nagaraj N, Mann M. 2014. Accurate

proteome-wide label-free quantification by delayed normalization and maximal peptide ratio extraction, termed MaxLFQ. Mol Cell Proteomics 13:2513–2526. https://doi.org/10.1074/mcp.M113.031591.
72. Tyanova S, Temu T, Cox J. 2016. The MaxQuant computational platform for mass spectrometry-based shotgun proteomics. Nat Protoc 11: 2301–2319. https://doi.org/10.1038/nprot.2016.136.
73. Herrero M, de Lorenzo V, Timmis KN. 1990. Transposon vectors containing non-antibiotic resistance selection markers for cloning and stable chromosomal insertion of foreign genes in gram-negative bacteria. J Bacteriol 172:6557–6567. https://doi.org/10.1128/jb.172.11.6557-6567.1990.
74. Hõrak R, Ilves H, Pruunsild P, Kuljus M, Kivisaar M. 2004. The ColR-ColS two-component signal transduction system is involved in regulation of Tn*4652* transposition in *Pseudomonas putida* under starvation conditions. Mol Microbiol 54:795–807. https://doi.org/10.1111/j.1365-2958.2004.04311.x.
75. Ainelo A, Tamman H, Leppik M, Remme J, Hõrak R. 2016. The toxin GraT inhibits ribosome biogenesis. Mol Microbiol 100:719–734. https://doi.org/10.1111/mmi.13344.
76. Hõrak R, Kivisaar M. 1998. Expression of the transposase gene *tnpA* of Tn*4652* is positively affected by integration host factor. J Bacteriol 180:2822–2829.
77. Wong SM, Mekalanos JJ. 2000. Genetic footprinting with *mariner*-based transposition in *Pseudomonas aeruginosa*. Proc Natl Acad Sci U S A 97:10191–10196. https://doi.org/10.1073/pnas.97.18.10191.
78. Kivistik PA, Putrinš M, Püvi K, Ilves H, Kivisaar M, Hõrak R. 2006. The ColRS two-component system regulates membrane functions and protects *Pseudomonas putida* against phenol. J Bacteriol 188:8109–8117. https://doi.org/10.1128/JB.01262-06.
79. Ojangu EL, Tover A, Teras R, Kivisaar M. 2000. Effects of combination of different-10 hexamers and downstream sequences on stationary-phase-specific sigma factor sigma(S)-dependent transcription in *Pseudomonas putida*. J Bacteriol 182:6707–6713. https://doi.org/10.1128/JB.182.23.6707-6713.2000.
80. Juurik T, Ilves H, Teras R, Ilmjärv T, Tavita K, Ukkivi K, Teppo A, Mikkel K, Kivisaar M. 2012. Mutation frequency and spectrum of mutations vary at different chromosomal positions of *Pseudomonas putida*. PLoS One 7:e48511. https://doi.org/10.1371/journal.pone.0048511.
81. Koch B, Jensen LE, Nybroe O. 2001. A panel of Tn7-based vectors for insertion of the gfp marker gene or for delivery of cloned DNA into Gram-negative bacteria at a neutral chromosomal site. J Microbiol Methods 45:187–195. https://doi.org/10.1016/S0167-7012(01)00246-9.
82. Tamman H, Ainelo A, Ainsaar K, Hõrak R. 2014. A moderate toxin, GraT, modulates growth rate and stress tolerance of *Pseudomonas putida*. J Bacteriol 196:157–169. https://doi.org/10.1128/JB.00851-13.
83. Jakovleva J, Teppo A, Velts A, Saumaa S, Moor H, Kivisaar M, Teras R. 2012. Fis regulates the competitiveness of *Pseudomonas putida* on barley roots by inducing biofilm formation. Microbiology 158:708–720. https://doi.org/10.1099/mic.0.053355-0.
84. Bao Y, Lies DP, Fu H, Roberts GP. 1991. An improved Tn7-based system for the single-copy insertion of cloned genes into chromosomes of gram-negative bacteria. Gene 109:167–168.